

Hole and Pair Structures in the t - J model

Steven R. White¹ and D.J. Scalapino²

¹*Department of Physics and Astronomy, University of California, Irvine, CA 92717*

²*Department of Physics, University of California, Santa Barbara, CA 93106*

(July 29, 2021)

Abstract

Using numerical results from density matrix renormalization group (DMRG) calculations for the t - J model, on systems as large as 10×7 , we examine the structure of the one and two hole ground states in ladder systems and in two dimensional clusters. A simple theoretical framework is used to explain why holes bind in pairs in two-dimensional antiferromagnets. For the case $J/t = 0.5$, which we have studied, the hole pairs reside predominantly on a 2×2 core plaquette with the probability that the holes are on diagonal sites greater than nearest-neighbor sites. There is a strong singlet bond connecting the spins on the two remaining sites of the plaquette. We find that a general characteristic of dynamic holes in an antiferromagnet is the presence of frustrating antiferromagnetic bonds connecting next-nearest-neighbor sites across the holes. Pairs of holes bind in order to share the frustrating bonds.

At low doping, in addition to hole pairs, there are two additional low-energy structures which spontaneously form on certain finite systems. The first is an undoped $L \times 2$ spin-liquid region, or ladder. The second is a hole moving along a one dimensional chain of sites. At higher doping we expect that hole pairing is always favored.

PACS Numbers: 74.20.Mn, 71.10.Fd, 71.10.Pm

Typeset using REVTeX

I. INTRODUCTION

The main obstacle to understanding two-dimensional doped antiferromagnets has been the inadequacy of current analytical and numerical tools when applied to these systems. A number of analytical approaches are available which work well in either high dimensions (such as dynamical mean field theory [1]) or one dimension (such as bosonization [2]), but not in two dimensions. Numerical approaches such as quantum Monte Carlo [3] and exact diagonalization [4–8] have been very useful, but quantum Monte Carlo suffers from a sign problem at low temperatures [9], and exact diagonalization can only be applied to small clusters.

Recently, however, density matrix renormalization group (DMRG) techniques have been developed which allow one to obtain accurate, detailed information about ground state expectation values on significantly larger clusters [10,11]. We have performed DMRG calculations on a variety of t - J clusters. We have been able to treat systems of width 3 and 4 at a variety of dopings, with lengths up to 32 sites. At low doping, we have results from wider systems, such as 10×7 . Here we examine the structure of the ground state of t - J clusters doped with one or two holes. Specifically, we have calculated the ground state expectation value of the spin S_i^z and the exchange field $\vec{S}_i \cdot \vec{S}_j$ around a dynamic hole or pair of holes. We have also calculated the spatial kinetic energy distribution of one or two holes in a cluster, the spatial kinetic energy distribution of one hole when a second hole has been projected onto a particular site, and the hole-hole correlation function in a two-hole state. From these calculations one obtains new insight into the nature of the structures holes can induce in an antiferromagnetic host and the origin of pair binding seen in some clusters. In a subsequent paper we will discuss the effect of additional holes and present results for pairing correlations on long two, three, and four chain ladders.

II. THEORETICAL FRAMEWORK

We first describe a simple theoretical framework for understanding hole motion in a t - J model. The Hamiltonian is [12]

$$\mathcal{H} = \mathcal{H}_S + \mathcal{H}_K = J \sum_{\langle ij \rangle} (\vec{S}_i \cdot \vec{S}_j - \frac{1}{4} n_i n_j) - t \sum_{\langle ij \rangle, s} P_G (c_{i,s}^\dagger c_{j,s} + c_{j,s}^\dagger c_{i,s}) P_G \quad (1)$$

where $\langle ij \rangle$ denotes nearest-neighbor sites, s is a spin index, \vec{S}_i and $c_{i,s}^\dagger$ are electron spin and creation operators, $n_i = c_{i,\uparrow}^\dagger c_{i,\uparrow} + c_{i,\downarrow}^\dagger c_{i,\downarrow}$, and the Gutzwiller projector P_G excludes configurations with doubly occupied sites. In the calculations shown here, we set the hopping $t = 1$ and the exchange $J = 0.5$.

Let $|\psi\rangle$ be the ground state of a particular t - J system with N sites and $N - m$ electrons. Define a hole projection operator for site i as $P_h(i) = c_{i,\downarrow} c_{i,\downarrow}^\dagger c_{i,\uparrow} c_{i,\uparrow}^\dagger$. $P_h(i)$ projects out the part of a wavefunction in which site i is vacant. Although we call this vacant site a ‘‘hole’’, there is not necessarily any spin associated with the vacancy: in the one dimensional t - J model, for example, there is not. A better term might be ‘‘dynamic vacancy’’, but the use of the term ‘‘hole’’ has now become fairly standard. In some systems, such as even-leg ladders, an extra spin-1/2 is bound to the vacant site, forming a composite object with charge and spin, which is sometimes called a ‘‘quasiparticle’’. We define an operator $P_h(h)$, which projects out a particular configuration of m holes, as $P_h(h) = P_h(h_1) \dots P_h(h_m)$, where $h = (h_1, \dots, h_m)$, and $h_1 < \dots < h_m$. We can then separate $|\psi\rangle$ into parts with specified hole locations as

$$|\psi\rangle = \sum_h P_h(h) |\psi\rangle = \sum_h a_h |\psi_h\rangle, \quad (2)$$

where $|\psi_h\rangle$ is a normalized wavefunction with holes at the specified sites, and $a_h > 0$. The ground state energy is given by

$$E = \sum_h a_h^2 \langle \psi_h | \mathcal{H}_S | \psi_h \rangle + \sum_h \sum_{h'} a_h a_{h'} \langle \psi_h | \mathcal{H}_K | \psi_{h'} \rangle. \quad (3)$$

The first term we refer to as the exchange energy, denoted by E_S . The second term in Eq. (3), the hopping energy or kinetic energy, can be written as

$$E_K = -t \sum_{\langle ij \rangle, s} \sum_h a_h a_{h'} \langle \psi_h | c_{i,s}^\dagger c_{j,s} | \psi_{h'} \rangle, \quad (4)$$

where the hole configurations h and h' are the same, except that h has a hole at site j and h' has one at site i . In general, we consider two hole configurations h and h' *adjacent* if they differ by a near-neighbor hop of a single hole. Define the hopping overlap between h and h' as

$$O_{h,h'} = \langle \psi_h | \sum_{\langle ij \rangle, s} (c_{i,s}^\dagger c_{j,s} + c_{j,s}^\dagger c_{i,s}) | \psi_{h'} \rangle. \quad (5)$$

Clearly a necessary condition for $O_{h,h'}$ to be nonzero is that h and h' are adjacent, in which case only one pair of sites i, j appears in the sum. If h and h' differ only in the position of hole m , $h_m \neq h'_m$, then

$$O_{h,h'} = \langle \psi_h | \sum_s c_{h'_m,s}^\dagger c_{h_m,s} | \psi_{h'} \rangle. \quad (6)$$

It is easy to see that $|O_{h,h'}| \leq 1$. The kinetic energy can be written as

$$E_K = -t \sum_{h,h'} a_h a_{h'} O_{h,h'} \quad (7)$$

We see that we can view the ground state as the result of a set of coupled variational calculations, where the exchange energy of each wavefunction $|\psi_h\rangle$ is minimized, subject to having as much overlap as possible with adjacent hole configurations. For $t > J$, the interplay between the kinetic and exchange terms is interesting. In the low doping regime, since there are more exchange terms which come into play, the bulk spin behavior is dominated by exchange. Close to any holes, however, since $t > J$, substantial modifications of the local spin arrangements can occur. At higher doping, the bulk spin behavior can be changed substantially as well.

Using DMRG, we can study $|\psi_h\rangle$ directly: we calculate $|\psi\rangle$, and then measure operators of the form $AP_h(h)$ (or $P_h(h)AP_h(h)$), normalizing by $\langle \psi | P_h(h) | \psi \rangle$. It is useful to use $A = \vec{S}_i \cdot \vec{S}_j$, where i and j are near a hole or pair of holes. This measurement gives us a “snapshot” of the spin configuration around a dynamic hole. If this expectation value

is close to -0.75 for two sites i and j , we say that there is a “singlet bond” connecting i and j , even if there is no term in the Hamiltonian directly coupling i and j . We use the terms “antiferromagnetic bond”, “valence bond”, or just “bond” simply to indicate that $\langle \vec{S}_i \cdot \vec{S}_j \rangle < 0$. Of course, Néel order makes weak “bonds” connecting widely separated sites on opposite sublattices, but we will be particularly concerned here with bonds connecting nearby sites on the *same* sublattice.

We can also take a snapshot of the spin configuration using $A = S_i^z$, for a single hole on an even number of sites. In that case, the ground state is degenerate with $S^z = \pm 1/2$, so that the expectation value of S_i^z in one of the ground states is finite. One can also project out some of the holes, and use $A = n_{i,s} = c_{i,s}^\dagger c_{i,s}$, to find out where the unprojected holes are, or $A = K_{ij} = -t \sum_s (c_{i,s}^\dagger c_{j,s} + c_{j,s}^\dagger c_{i,s})$, to study their motion.

III. RESULTS

The results in this paper were all calculated using the finite system version of DMRG [10], keeping track of transformation matrices to construct the initial guess for each superblock diagonalization [11]. From 200 to 800 states were kept per block, with 800 states necessary for the 10×7 system. We performed hundreds or thousands of measurements for each system. Ordinarily storing all the operators needed to measure so many quantities would greatly increase the memory used by the program, but since the transformation matrices contain a complete description of the approximate wavefunction produced by the DMRG algorithm, the measurements could be performed at the end of the calculation, in manageable groups of 50 to 100. The large number of measurements, at worst, doubled or tripled the computation time.

A. Single chain

As a warmup exercise, consider the 1D t - J model, with one hole. One might consider as a variational ansatz for $|\psi_h\rangle$ a Néel arrangement of the electron spins, with one electron

removed. In this ansatz we have made a “quasiparticle”, since an extra spin $1/2$ is associated with the hole. However, this is a very poor ansatz: $|\psi_h\rangle$ has no overlap with $|\psi_{h\pm 1}\rangle$. Alternatively, one can arrange the spins as shown in Fig. 1(a), with shifted Néel arrangements separated by the hole [13]. There are two spin wavefunctions $|\psi_h\rangle$, plus translations: for h odd (even), an up spin is to the left of the hole, while for h even (odd), a down spin is to the left of the hole. In this case there is complete overlap, and the kinetic energy associated with the hole takes on the maximal (in magnitude) value $-2t$. This is a simple intuitive argument for spin–charge separation in a 1D t - J model. Since a single hole moves freely, it also suggests that there is no kinematic reason for the binding of pairs of holes, although for unphysically large J/t the diagonal term in Eq.(3) can cause binding.

A justification for considering these Néel configurations for the 1D t - J model is the existence of power-law decaying antiferromagnetic correlations in the 1D Heisenberg model. Bond-bond correlations $\langle \vec{S}_i \cdot \vec{S}_{i+1} \vec{S}_j \cdot \vec{S}_{j+1} \rangle$ also decay as a power law, suggesting a valence bond configuration as a complementary ansatz: valence bonds occupy odd (even) links to the left of the hole, and even (odd) links to the right, as shown in Fig. 1(b). If one takes this configuration, and applies $\sum_s c_{i,s}^\dagger c_{j,s}$ to move the hole to a neighboring site, one obtains the configuration in Fig. 1(c), with a valence bond straddling the hole. Consequently, if we let the valence bond configuration of Fig. 1(b) define $|\psi_h\rangle$ for all odd sites h , and let the configuration of Fig. 1(c) define $|\psi_h\rangle$ for all even sites, then the hole moves freely, with the kinetic energy taking on its maximal value $-2t$.

In Fig. 1(d)-(e), we show DMRG results for the bond strength $A = \vec{S}_i \cdot \vec{S}_j$ for a single hole in a 15 site 1D chain, with open boundary conditions. The width of the line corresponding to each bond has been made proportional to the bond strength, as indicated by the scale in the box. The maximum possible bond strength is $-3/4$. The boundaries induce dimerization in the system, and the results are quite similar to the valence bond configurations shown in Fig. 1(b)-(c). It is also possible to obtain results which look like Fig. 1(a). In Fig. 1(f), we show results for the $S^z = 1/2$ ground state of a system with an even number of sites and one hole. The excess spin $1/2$ is spread out over the lattice.

Particularly interesting is the strength of the bond across the hole in Fig. 1(e). In order to maximize the hopping overlap with adjacent hole configurations, in addition to having antiferromagnetic correlations on nearest-neighbor links, we expect such correlations between *next-nearest-neighbor* sites i and j if there is a hole at site k which is a nearest-neighbor to both i and j . Such a valence bond becomes a nearest-neighbor link after one hop of the hole to either site, since moving the hole also moves the bond. For example, suppose the hole configuration h has a hole at site k , with i and j nearest-neighbor sites to k . Let h' be the hole configuration after the hole hops from k to i . Since j and k are nearest-neighbor sites, we expect a strong antiferromagnetic bond between these sites in $|\psi_{h'}\rangle$. In order to maximize the hopping overlap $O_{h,h'}$, there will also be a strong antiferromagnetic bond between sites i and j in $|\psi_h\rangle$. This tendency applies to two dimensions as well as one, and appears as an essential ingredient for pair binding in ladders and two dimensions.

B. Two chains

We now consider a two chain ladder system, with identical couplings along the legs and rungs, $t = 1$ and $J = 0.5$. We consider first a single hole. In Fig. 2(a) we show bond strengths in $|\psi_h\rangle$ in the vicinity of the dynamic hole for a 32×2 lattice, with h on site $(16, 1)$. As we argued above, the system has a tendency to form antiferromagnetic correlations on next-nearest-neighbor sites around the hole. Except in one dimension, this tendency introduces *frustration*, since sites on the same sublattice tend to be parallel. A single Heisenberg spin chain becomes dimerized for sufficiently large frustrating next-nearest neighbor interaction ($J' > 0.24J$). Similar dimerization is clearly evident in the two bonds above the hole Fig. 2(a). The dimerization weakens one of the nearest-neighbor bonds around the hole sufficiently to allow two of the next-nearest-neighbor links to form antiferromagnetic correlations. Since the hole is not quite at the center of the system, the figure need not be symmetric.

A single Heisenberg spin chain with frustrating next-nearest neighbor interaction $J' >$

$0.5J$ develops incommensurate, spiral spin correlations, in addition to dimerization [14–16]. We have looked for this in $|\psi_h\rangle$ by measuring $(\vec{S}_i \times \vec{S}_j) \cdot (\vec{S}_k \times \vec{S}_l)$, where the hole was on site (16,1) and the spin operators $i, j, k,$ and l were for sites (15,1), (15,2), (17,2), and (17,1), respectively. No enhancement of this quantity by the presence of the hole was found, nor was any found in the other lattices we studied here. However, it still might occur [17] in other parameter regimes, such as $t \gg J$.

Unlike the single chain Heisenberg model, the undoped two chain ladder does not have gapless spin 1/2 excitations. Spin-charge separation does not occur in the two chain ladder, and an extra up or down spin is bound to a single hole, forming a quasiparticle. It is not possible to specify a precise location for the extra spin, since every spin fluctuates between up and down, but one can get some indication of its whereabouts by measuring $\langle \psi_h | S_i^z | \psi_h \rangle$. In Fig. 2(b) we show this quantity for the same $|\psi_h\rangle$ shown in Fig. 2(a), in which the extra spin points up. Clearly the extra spin is localized close to the hole, spending most of the time on the same rung as the hole. Short-range antiferromagnetic correlations cause $\langle S_i^z \rangle$ to be negative for some of the nearby sites.

In Fig. 2(c)-(d) we show similar results for a *static* hole [18]. In this case we remove one site, find the ground state, and measure its properties. In Fig. 2(c) we see that there is no dimerization of the bonds above the vacancy, and no antiferromagnetic correlations between next-nearest-neighbor sites. In Fig. 2(d), we see that the extra spin is still mostly on the same rung as the static hole, but there is substantially more antiferromagnetic polarization caused by the extra spin. For a dynamic hole, this polarization is mostly absent because it reduces the overlap between adjacent hole configurations, since it is tied to the hole location.

The addition of a static hole increases the total exchange energy of the system, including the $-\frac{1}{4}Jn_in_j$ term, by $0.995t = 1.99J$. The frustrating effects of a dynamic hole further increase the total exchange energy by $0.26t$, but the kinetic energy associated with the dynamic hole is $-2.37t$.

Next we consider the two chain system with two holes, which bind to form a pair. In Fig. 3(a) we show the expectation value of the kinetic energy on each bond, when the

location of only one of the holes has been specified with the projection operator $P_h(h)$. This provides information not only on where the other hole is, but between which sites it hops the most. We see that the other hole spends most of its time on the opposite chain, close to the first hole. What fraction of the time the other hole spends on each of the sites is obtained from $\langle \psi | P_h(h) | \psi \rangle$ with both locations specified. We find if the first hole is at (16,1), the probability for finding the other on (15,2), (16,2), or (17,2), is about 0.15, for (14,2) or (18,2), about 0.075, and for (15,1) or (17,1), about 0.055. The second hole spends more total time on the *two* sites a distance $\sqrt{2}$ away from the first hole than on the *three* nearest-neighbors sites. The probability is over 0.99 that the other hole is within a distance of 6 of the first hole.

Hole-hole density correlation functions have been calculated using Lanczos methods for two holes on clusters ranging from 4×4 [4,5] up to $\sqrt{26} \times \sqrt{26}$ [8], and using Green's function Monte Carlo techniques on an 8×8 cluster [19]. It has been estimated that J/t must be larger than 0.27 for pair binding to occur [19]. Near-neighbor and next-nearest-neighbor diagonal hole-hole correlations are dominant for $J/t > 0.4$. Based on the $\sqrt{26} \times \sqrt{26}$ results [8], for $J/t = 0.5$ the holes are about 20% more likely to be found across a diagonal than on near-neighbor sites. For J/t greater than about 1.0, the near-neighbor correlation exceeds the diagonal one.

In Fig. 3(b)-(d) we show the bond strengths when the dynamic holes are in three possible configurations. The exchange energy of $|\psi_h\rangle$, compared to the system without holes, is $1.45t$ for (b), $1.71t$ for (c), and $1.92t$ for (d). Despite these energies, the system spends as much time in configuration (d) as in (b), and much more time in either of these than in (c). Configuration (d) is favored, despite its high exchange energy, because it connects with more hole configurations h' than does (b) or (c), giving it more weight in the kinetic part of the energy. There are six configurations h' connected to (d), but only four to (b) or (c) (counting hops of either hole).

Perhaps the most remarkable aspect of Fig. 3 is the very strong next-nearest-neighbor singlet bond crossing the holes in Fig. 3(d). For four of the six hops available to (d), this

bond becomes a nearest-neighbor bond, and in each of those neighboring configurations the bond is quite strong. Therefore, the kinetic term strongly favors a singlet bond connecting these sites.

On the 32×2 system, the kinetic energy of a pair of holes is -4.57, compared with -4.74 for two separate holes. The increase in exchange energy caused by a pair of holes is 2.06, compared with 2.51 for two separate holes. Thus the slight increase in kinetic energy from binding a pair of holes is more than made up for by a substantial decrease in exchange energy. The pair binding energy, defined as

$$E_b = 2E(1) - E(2) - E(0), \quad (8)$$

where $E(m)$ is the ground states energy with m holes, is $E_b = 0.28$.

It is useful to define the *frustration energy* associated with a particular hole configuration h as

$$E_f(h) = \langle \psi_h | \mathcal{H}_S | \psi_h \rangle - \langle \psi_{h,static} | \mathcal{H}_S | \psi_{h,static} \rangle, \quad (9)$$

where $|\psi_{h,static}\rangle$ is the ground state in the static hole configuration h . The frustration energy of two separate holes on the 32×2 is $0.52t$. For two holes in configurations (b), (c), and (d), the frustration energies are $0.077t$, $0.249t$, and $0.066t$, respectively, much less than for separate holes. The frustration energy associated with the strong diagonal frustrating bond in (d) is rather small. This reflects the fact that a free $S = 1/2$ forms on the end of a two chain Heisenberg ladder with one extra site on one chain [20], and this extra spin can be used to form the diagonal singlet bond.

C. Three chains

We next consider a three chain ladder system with a single hole. In Fig. 4(a) we show the kinetic energy on each link in a 16×3 system, for sites near the center of the system. It is clear that the hole resides mostly on the outer legs, and that when it does hop onto

a center-leg site, it is most likely to then hop to an outer leg. In Fig. 4(b) we show the exchange energy on each link near a mobile hole in the state $|\psi_h\rangle$ with h on an outer leg near the center of the system. The expected next-nearest neighbor antiferromagnetic bond has formed across the hole. The dimerization is quite different than in the two-chain case: it forms in the vertical direction, where it is both more effective at accomodating the frustration and less costly in energy. The dimerized bonds form a structure resembling a short two-leg ladder. In Fig. 4(c) we show similar results for the hole on the adjacent center-leg site. A particularly strong singlet bond forms across the hole, reflecting a strong tendency to hop vertically. Fig. 4(d) shows $\langle S^z \rangle$ on sites about the hole of Fig. 4(b). The pattern strongly resembles that of a single chain. Instead of being localized near the hole, the extra $S = 1/2$ is distributed about the system, indicating spin-charge separation. The spins form a one-dimensional shifted-Néel configuration. On the same leg as the hole, the other two sites are bound tightly into a singlet, and $\langle S^z \rangle$ is very small. Fig. 4(e) shows similar results for the hole on the center leg. The frustration energy of a single hole on an outer leg on three chains is $0.19t$, and on the center leg, $0.68t$.

Two holes on a long three-chain ladder with $J/t = 0.5$ are not bound. The density of holes has two widely spaced broad peaks. Fig. 4(f) shows the kinetic energy of one hole when the other hole is projected onto a site at one of the peaks in the density. Direct measurement of the hole-hole correlation function shows that the hole is found exactly where the kinetic energy is large.

Why are two holes bound on two chains and not on three chains? This is what one would expect based on arguments using an RVB variational ansatz for the background spin system [20]. However, those arguments are based on a static treatment of holes, and as we have seen here, for $J/t = 0.5$ the holes cannot be treated statically. The RVB ansatz, as well as various analytical approaches [21,22], predicts the existence of free spinon excitations on ladders with odd numbers of legs, and this is important. In the three chain system a hole can separate into a hole and a free, zero-energy spinon, which one would expect to have lower energy. It is interesting to compare Fig. 4(b) and Fig. 2(a): on three chains, a low energy

local spin structure can form involving vertical dimerization which allows easy hopping. On two chains, vertical dimerization is not possible, and the bonds above the hole also carry the extra $S = 1/2$, reducing their strength. Direct comparison of the energies supports this picture: on a 16×3 system, adding one hole (and spinon) increases the exchange energy by $1.19t$, and decreases the kinetic energy by $2.54t$. On a 16×2 system, the exchange energy is increased by $1.26t$ and the kinetic energy decreases by $2.36t$. By this measure a pair of separated holes is lower in energy on three chains by $0.50t$. The pair binding energy on the two chain system is $0.28t$, less than the difference in hole energy between two and three chains.

D. Four chains

We now consider a four chain ladder system with a single hole. Unlike the three chain case, the probability of finding the hole on the center two chains is about the same as finding it on an outer chain. This is despite the fact that only three bonds are broken when the hole is on an outer chain, versus four for an inner chain. In Fig. 5(a,b) we show the bond strengths about a dynamic hole on an outer chain and on an inner chain. Next-nearest-neighbor antiferromagnetic bonds have formed across the hole. Dimerization is also present. The frustration energy of the hole locations shown in Fig. 5(a) and (b) are $0.26t$ and $0.42t$, respectively. The additional spins surrounding the hole, compared to two or three chains, tend to reduce both horizontal and vertical dimerization. The precise pattern of frustrating bonds and dimerization is somewhat complicated. One could imagine putting in a static vacancy and including next-nearest-neighbor interactions J' about the vacancy to approximate the effect of hole motion. This approach neglects the ability of the hole to hop preferentially between some pairs of sites in order to adapt to the frustration. This effect is visible in Fig. 5(b), where the hole prefers to hop vertically rather than horizontally, and the vertical frustrating bond is stronger.

In Fig. 5(c,d) we show the same results, but with the undoped spin background sub-

tracted off. This indicates more clearly the distortion caused by the hole. Notice that all the bonds immediately surrounding the hole are weaker. In Fig. 5(e,f) we show the same results for static holes (vacancies). The distortion of the spin background for static holes is much smaller, and for the bonds immediately surrounding the hole, opposite in sign. The static hole induces no dimerization or frustration.

We now consider two holes on a four chain ladder. In Fig. 6 we show the expectation value of the kinetic energy on each bond, when the location of only one of the holes has been specified with the projection operator $P_h(h)$. It is clear that the two holes are bound. However, the precise pattern of hopping initially seems rather strange. The patterns primarily reflect the fact that an *undoped* two-leg ladder configuration of spins is a low energy configuration. One can compare undoped ladders with even numbers of legs, which have a spin gap, and odd numbers of legs, which are gapless. It is natural to expect that the gap comes about both by a rise in the spin excitation energy *and* a lowering in the “vacuum” ground-state energy. Thus we expect a two chain undoped ladder, which has a very large gap of about $0.5J$, to be an especially low energy system in some sense. Hence the two holes in Fig. 6 prefer to lie on either the top two legs or the bottom two legs, or the top and the bottom legs, but not on the first and third, second and third, or second and fourth. If a hole is on the “wrong leg”, it especially doesn’t like to hop horizontally.

A four chain undoped system will also have low energy, since it too has a spin gap. Tsunetsugu, et. al. [23] have argued that this can lead to striped phases in which one dimensional lines of holes divide ladders with even numbers of legs. Our results clearly indicate that both single holes and pairs of holes often arrange their motion so that undoped two-leg ladder-like arrangements of spins can form. The tendency toward formation of four-leg ladder structures is weaker.

The three chain results can also be interpreted in terms of ladder formation, in that the holes predominantly sit on the outer legs, with the other two legs near each hole forming an undoped two chain system. An important difference between the structures we see and those suggested by Tsunetsugu, et. al., is in the density of holes or pairs of holes adjacent

to the ladders: we see quite low densities, while they suggested a line of holes with density near unity.

In Fig. 7 we show the bond strengths about the two most probable hole configurations, which are almost equally probable. In (a) we see the strong next-nearest neighbor diagonal singlet bond crossing the holes. Horizontal hopping transforms this diagonal bond into vertical bonds which sit on each side of the pair, as seen in (b).

The kinetic energy of a pair of holes is $-5.16t$, compared with $-5.25t$ for two separate holes. The increase in exchange energy caused by a pair of holes is $2.47t$, compared with $2.78t$ for two separate holes. As in the two-chain case, the slight increase in kinetic energy from binding a pair of holes is more than made up for by the decrease in exchange energy. The pair binding energy is $E_b = 0.21t$. This pair binding energy is smaller by 25% than the two chain value. In contrast, the spin gap for the undoped four chain system is smaller by over 60% compared to two chains. The frustration energy corresponding to Fig. 7(a) is $0.20t$. For Fig. 7(b), it is $0.14t$. The frustration energy of two separate holes would be $0.51t$ if they were both on outer legs, and $0.68t$ if one was on an outer leg and one on an inner leg.

E. Five chains

We now consider a five chain ladder system with a single hole. Recall that a single hole on a three chain ladder spent most of the time on an outer chain. Since the undoped three and five chain systems have similar, gapless ground states, one might expect a hole on the five chain system to spend more time on an outer chain than in the center. However, this is not the case. In Fig. 8(a) we show the kinetic energy for a single hole on an 8×5 cluster. The hole spends most of the time on the center chain. By moving on the center chain, the system is divided into two undoped two-chain ladder systems above and below the hole. As Fig. 8(b) shows, this configuration allows the vertical dimerization found in the three chain system to form both above and below the hole, allowing a strong frustrating bond to form horizontally across the hole. The hole tends not to hop all the way to the ends of the system

so that vertical two-chain structures can form there. The frustration energy at site (4,3) is $E_f = 0.26t$. In Fig. 8(c), the corresponding spin configuration is shown. The same shifted Néel pattern found in three chains is again seen, with the spins on an entire five-site rung shifting with the motion of the hole.

Two holes in this system repel. The spin configuration around a single hole is highly favorable, as in the three chain case. The “core” of a bound pair of holes is a 2×2 plaquette. If a pair were to form, it would divide the system into a two chain ladder and a single chain, and the single chain would have high energy. In fact, the separate holes form the structure shown in Fig. 9(a), where the system is divided into ladders both horizontally and vertically! In Fig. 9(b), we show the kinetic energy of one of the holes when the other is projected onto a site. The holes clearly are unbound. The system dimerizes vertically above and below each hole, and horizontally to the left and right of each hole.

The vertical hopping patterns are highly dependent on the length of the system. An 8×5 system with two holes allows convenient division of the system into width-two pieces in both directions. In Fig. 9(c,d), we show the results similar to those shown in Fig. 9(a,b) but for a 10×5 system. In this case, some of the vertical pieces must be of width greater than two. In Fig. 9(d), we see that when the first hole is on site (3,3), the motion of the second holes divides the right part of the system into either two horizontal two-chain ladders or into a vertical two-chain and a vertical four-chain ladder.

F. A 8×6 cluster

We now consider an 8×6 cluster with a single hole. In Fig. 10(a) we show the kinetic energy per bond for the hole. A single hole is likely to be found in the central sites of the cluster, allowing a two leg ladder to run along the entire edge of the system. Some slight asymmetry is visible in the figure; this is a result of a slight numerical inaccuracy in the DMRG calculation. We kept 600 states per block in this calculation; despite this many states, the truncation error (also referred to as the discarded weight) was relatively

high: about 6×10^{-5} . This level of accuracy was, however, sufficient to determine the general structure of the hole. In Fig. 10(b) we show the bond strengths about the hole projected onto a central site. Next-nearest-neighbor antiferromagnetic bonds have formed across the hole, but they are somewhat weaker than in the narrower systems. This reflects a decreased ability to hop in this system, which is dominated more by the exchange energy. Dimerization is also present, particularly beneath the hole, but it is also weaker than in the narrower systems. In Fig. 10(c), we show the difference in bond strength between the one hole system and the undoped system. The distortion caused by the hole is fairly substantial over a 5×5 region. All the bonds immediately surrounding the hole are weaker. In Fig. 10(d) we show the same results for a static hole. The distortion of the spin background is much smaller than for a dynamic hole (note the decreased scale), and for the bonds immediately surrounding the hole, opposite in sign. The frustration energy for this hole location is $E_f = 0.29$.

In Fig. 11 we show results for two holes on an 8×6 cluster. Again we kept 600 states per block, but the truncation error was higher than in the single-hole calculation: 2×10^{-4} . This was still sufficient to determine the structure of the pair with reasonable accuracy and to determine the pair binding energy. In Fig. 11(a) we show the expectation value of the kinetic energy of a hole, when the other hole has been projected onto a central site. The two holes are clearly bound. The hole is somewhat more likely to be to the left of the projected hole than one might expect; however, this configuration breaks the system vertically into two-chain and four-chain undoped ladders, rather than two three-chain undoped ladders.

In Fig. 11(b-d) we show the bond strengths surrounding several likely configurations of the pair. The frustrating diagonal singlet crossing the pair is clearly present in Fig. 11(b): this is the clearest “signature” of a bound pair of holes, and is present in all the systems in which we have found pair binding. In addition, additional frustrating bonds crossing the holes are present in both directions. Vertical dimerization is present above and below the holes, where it is expected, and to the left and right, where we might have expected horizontal dimerization. Even on a system of width 6, the boundaries are still

substantially affecting the spin structure surrounding the pair, and it is not clear which type of dimerization would appear in a large system. The most probable configuration of the pair is not shown: (3,4)-(4,3), with probability 0.018. Configuration (b), (c), and (d) have probabilities of 0.014, 0.005, and 0.017, respectively. The frustration energies $E_f(h)$ for configurations (b), (c), and (d) are $0.32t$, $0.54t$, and $0.20t$, respectively. The frustration energy of two separate holes is $0.58t$.

In Fig. 11(e,f) we show the difference in bond strengths of the two-hole system and the undoped system. Substantial distortion of the spin structure occurs over a 6×6 region.

The kinetic energy of a pair of holes on an 8×6 cluster is $-5.36t$. Twice the kinetic energy of a single hole is $-5.38t$. The increase in exchange energy caused by a pair of holes is $2.71t$, compared with $2.96t$ for two separate holes. The increase in kinetic energy from binding a pair of holes is very tiny, and is more than made up for by the decrease in exchange energy. The pair binding energy is $E_b = 0.24(2)t$. This pair binding energy is slightly bigger than on a 16×4 lattice.

G. 8×7 and 10×7 clusters

We have performed a few DMRG studies of width 7 systems. We studied a 10×7 cluster with two holes, keeping 800 states per block, with a total of 10 sweeps through the lattice. The truncation error was fairly large, 2×10^{-4} , but it was clear that the two holes were bound, and tended to stay near the center of the cluster. In general, the results were similar to the 8×6 cluster. We also studied a 8×7 cluster with a staggered magnetic field $H = 0.15$ applied to the edge sites. The idea was to simulate the Néel spin background of an infinite undoped lattice. The field strength was chosen to represent a mean field coupling to surrounding sites, each with an average magnetization of $\langle S_i^z \rangle = 0.3$. Again, two holes were bound, with a pair binding energy of about 0.15.

H. A 2×2 cluster

The bound pair of holes which have been found in a number of these clusters are characterized by a 2×2 core region over which the dominant hole-hole correlations occur. In order to better understand this core we consider the 2×2 lattice shown in Fig. 12.

Introducing the singlet valence bond operator between sites i and j

$$\Delta_{ij}^\dagger = \frac{1}{\sqrt{2}}(c_{i,\uparrow}^\dagger c_{j,\downarrow}^\dagger + c_{j,\uparrow}^\dagger c_{i,\downarrow}^\dagger), \quad (10)$$

the ground state of the undoped half-filled system can be written as

$$|\psi\rangle_0 = N_0[\Delta_{14}^\dagger \Delta_{23}^\dagger - \Delta_{12}^\dagger \Delta_{34}^\dagger]|0\rangle, \quad (11)$$

with $|0\rangle$ the vacuum. The ground state of the two-hole system is

$$|\psi\rangle_2 = N_2[a(\Delta_{12}^\dagger + \Delta_{23}^\dagger + \Delta_{34}^\dagger + \Delta_{14}^\dagger) + b(\Delta_{13}^\dagger + \Delta_{24}^\dagger)]|0\rangle, \quad (12)$$

with $a = 1$ and $b = [2 + (J/4t)^2]^{1/2} - J/4t$. In the doped, two-hole state $|\psi\rangle_2$, the ratio of the edge singlet (e.g. 1-2) to diagonal singlet (e.g. 1-3) amplitude is

$$\frac{a}{b} = \frac{1}{[2 + (J/4t)^2]^{1/2} - J/4t}. \quad (13)$$

For $J/t = 2$, this ratio is unity. For $J/t < 2$, the diagonal amplitude is larger than the edge amplitude. This is reflected in the t - J results previously discussed, where for $J/t = 0.5$ the hole-hole correlations were found to be larger for next-nearest-neighbor diagonal sites than for nearest-neighbor sites.

The ground state, Eq. (11), of the undoped 2×2 system transforms as $d_{x^2-y^2}$, while the two-hole state, Eq. (12), transforms as an s -wave. Thus the hole-pair creation operator that connects $|\psi\rangle_0$ to $|\psi\rangle_2$ must transform as $d_{x^2-y^2}$ [24,25]. A simple nearest-neighbor operator of this form is

$$\Delta = \Delta_{14} - \Delta_{12} + \Delta_{23} - \Delta_{34}. \quad (14)$$

Applying this to the undoped ground state $|\psi\rangle_0$ given by Eq. (11), one finds that

$$\Delta|\psi\rangle_0 = -2N_0[\Delta_{12}^\dagger + \Delta_{23}^\dagger + \Delta_{34}^\dagger + \Delta_{14}^\dagger]|0\rangle. \quad (15)$$

This clearly has a nonzero overlap with the two-hole ground state $|\psi\rangle_2$, but it does not contain the diagonal singlet parts. However, if we were to “time-evolve” this state towards the two-hole ground state by applying $e^{-\mathcal{H}\tau}$ we would have for short imaginary times τ

$$e^{-\mathcal{H}\tau} \Delta|\psi\rangle_0 \approx (1 - \mathcal{H}\tau)\Delta|\psi\rangle_0, \quad (16)$$

and the hopping kinetic energy in \mathcal{H}_K generates the diagonal singlet terms

$$\mathcal{H}_K \Delta|\psi\rangle_0 \sim t(\Delta_{13}^\dagger + \Delta_{24}^\dagger)|0\rangle. \quad (17)$$

An improved hole pair creation operator would include, in addition to Δ , terms of the form $\mathcal{H}_K \Delta$.

A $d_{x^2-y^2}$ hole pair creation operator, generalized to include holes on next-nearest-neighbor diagonal sites, has been discussed by Poilblanc [8]. One can expand a generalized hole-pair creation operator in terms of operators which create a pair of holes on sites separated by a distance R . For our 2×2 cluster this involves

$$\Delta_{d_{x^2-y^2}} = \sum_R \Delta_R, \quad (18)$$

with $R = 1$ and $R = \sqrt{2}$. The nearest-neighbor operator Δ_1 is just the operator given in Eq. (14). As discussed by Poilblanc, a next-nearest-neighbor term possessing $d_{x^2-y^2}$ symmetry is

$$\Delta_{\sqrt{2}} = (\vec{S}_1 - \vec{S}_3) \cdot \vec{T}_{24} - (\vec{S}_2 - \vec{S}_4) \cdot \vec{T}_{31}, \quad (19)$$

with

$$\vec{S}_1 \cdot \vec{T}_{24} = \frac{1}{2}(c_{1\uparrow}^\dagger c_{1\uparrow} - c_{1\downarrow}^\dagger c_{1\downarrow})(c_{2\uparrow} c_{4\downarrow} - c_{4\uparrow} c_{2\downarrow}) + c_{1\uparrow}^\dagger c_{1\downarrow} c_{2\uparrow} c_{4\uparrow} + c_{1\downarrow}^\dagger c_{1\uparrow} c_{2\downarrow} c_{4\downarrow}. \quad (20)$$

Note that since $\vec{T}_{24} = -\vec{T}_{42}$, Eq. (20) has $d_{x^2-y^2}$ symmetry. Acting on the undoped ground state, $\Delta_{\sqrt{2}}$ generates the diagonal singlets

$$\Delta_{\sqrt{2}}|\psi\rangle_0 \sim (\Delta_{13}^\dagger + \Delta_{24}^\dagger)|0\rangle. \quad (21)$$

The action of this operator on $|\psi\rangle_0$ is the same as $\mathcal{H}_K\Delta$.

Based on this, we believe that the bound hole pairs observed in various clusters should be thought of as $d_{x^2-y^2}$ pairs. The diagonal-singlet bond as well as the nearest-neighbor singlet bonds reflect the two-hole structure of Eq. (12). In the larger clusters the pair structure is more extended, corresponding to further operations of $(1 - \mathcal{H}\tau)^N$ on $\Delta|\psi\rangle_0$, Eq. (16), or longer-range operators Δ_R in Eq. (18). The pair structure on larger systems includes both larger separation of the holes and alterations of the spin background near the pair.

IV. DISCUSSION

In considering one and two hole ground states of a wide variety of clusters, we have found a remarkable sensitivity to the shape of the cluster. Underlying the variety of results, however, are a few basic low-energy structures. The nature of the ground state of any particular system is based on which arrangement of these basic structures is lowest in energy.

The most important structure is a bound pair of holes. This structure allows the pair to hop rather freely in order to decrease the kinetic energy, without disrupting the spin background more than necessary. The bound pair is characterized by a 2×2 “core” region discussed above. Surrounding the core and extending several lattice spacings further is a region in which the spin structure is strongly perturbed. Within the core, for the case $J/t = 0.5$ which we have studied, the pair of holes is more likely to be at next-nearest-neighbor diagonal sites than nearest-neighbor sites, in order to maximize the hopping overlap with other hole configurations. When the two holes are diagonally situated, a strong singlet bond is present across the other two sites of the core. This singlet becomes a strong nearest-neighbor singlet bond after one of the holes hops next to the other. The singlet forms in order to maximize the hopping overlap with these other hole configurations. In order to respond to this frustrating bond, and to other weaker frustrating bonds across each of the holes, the surrounding spins dimerize, reducing the spin-spin correlations around the pair.

The effect of this dimerization is to induce a “spin-liquid” region surrounding the pair.

Frustrating next-nearest-neighbor bonds forming across holes are a universal feature in all of the clusters we have studied. These bonds are necessary for hole motion. Holes bind in pairs in order to share their frustration. This mechanism for pairing is quite different from simple “broken-bond” counting, which predicts nearest-neighbor pairing for *static* holes: for two static holes, a nearest neighbor configuration eliminates seven bonds, while anything else eliminates eight. For physical values of J/t , such as $J/t = 0.5$, the “broken-bond” effect enhances pair-binding somewhat, but is not dominant. Consider once again the 8×6 cluster, with two holes. Results for the hole-hole correlation function indicate that the pair resides on nearest-neighbor sites only 22% of the time. Even if a broken bond results in an extra exchange energy of $J = 0.5$, the effect on pair binding is only $0.22J = 0.11t$, while the actual pair binding energy is $0.24(2)t$. A more accurate estimate of the effect of broken bonds comes from considering two *static* holes on an 8×6 cluster: the difference in energy between nearest-neighbor static holes and widely separated holes is $0.62J$, rather than J , suggesting that the broken-bond energy for dynamic holes is about $0.07t$. In contrast, the frustration energy for two bound holes in the most probable hole configurations ranges from $0.25t$ - $0.40t$ *less than* the frustration energy of two separate dynamic holes.

The next most important structure is a nearly undoped two-leg ladder region. The large spin gap of a two-leg ladder coincides with a low energy spin-liquid ground state. The two-leg ladder is dimerized, in that the rung bonds are stronger than the leg bonds. This makes the ladder especially suited for a hole or pair of holes to move beside it.

Usually when ladder structures form, they are bounded by regions with pairs. In the special case of a five-leg ladder, pairs of holes are too wide, and the system instead has unpaired holes moving in one dimension, breaking the system into two-leg ladders. This is the last important structure: a one-dimensional line of unpaired holes. This structure is low enough in energy that it can appear in order to allow the formation of one or two undoped two-leg ladders, specifically in the three and five chain systems.

The energy difference between these structures is sufficiently small that modest external

perturbations can lead to the trapping of holes or the formation of static even-leg ladders. Even in the absence of external perturbations, we would expect that a dilute concentration of holes will give rise to fluctuating extended structures in the medium. Although we have not presented results here for more than two holes, we have such results for three, four, and five chains and will present them elsewhere. Based on our results at finite doping, we believe that the tendency to form two-leg ladders persists into the finite, but low doping regime, while at moderate doping, ladders diminish in importance and pairs of holes dominate. The even-leg ladders that are present in the dilute system could give rise to the pseudo-gap observed in the underdoped cuprates. It has been suggested that holes doped into the t - J model will phase separate [26]. However, in our studies with more holes, we find no evidence for phase separation at $J/t = 0.5$, which is consistent with previous t - J studies on clusters up to $\sqrt{26} \times \sqrt{26}$, in which phase separation was found only at larger J/t values [8]. The ladder structures we find are not the result of a competition between phase separation and a long-range Coulomb interaction [27], but arise directly from the short-range interactions in the t - J model.

ACKNOWLEDGEMENTS

We acknowledge support from the from the NSF under Grant Nos. DMR-9509945 and DMR95-27304. Some of the calculations were performed at the San Diego Supercomputer Center.

REFERENCES

- [1] W. Metzner and D. Vollhardt, Phys. Rev. Lett. **62**, 324 (1989); A. Georges and G. Kotliar, Phys. Rev. B **45**, 6479 (1992); M. Jarrell, Phys. Rev. Lett. **69**, 168 (1992); A. Georges, G. Kotliar, W. Krauth, and M. J. Rozenberg, Rev. Mod. Phys. **68**, 13, (1996).
- [2] D.C. Mathis and E.H. Lieb, J. Math. Phys. **6**, 304 (1965); A. Luther and V.J. Emery, Phys. Rev. Lett. **33**, 589 (1974); H. Frahm and V. Korepin, Phys. Rev. B **42**, 10553 (1990).
- [3] D.J. Scalapino, *Perspectives in Many-Particle Physics*, R.A. Broglia, J.R. Schrieffer, and P.F. Bortignon, eds. (North Holland, 1994) 95-125.
- [4] J. Bonca, P. Prelovsek, and I. Sega, Phys. Rev. B **39**, 7074 (1989).
- [5] Y. Hasegawa and D. Poilblanc, Phys. Rev. B **40**, 9035 (1989).
- [6] E. Dagotto, J. Riera, and A.P. Young, Phys. Rev. B **42**, 2347 (1990).
- [7] P. Prelovsek and X. Zotos, Phys. Rev. B **47**, 5984 (1993).
- [8] D. Poilblanc, Phys. Rev. B **49**, 1477 (1994).
- [9] E.Y. Loh, et.al., Phys. Rev. B **41**, 9301 (1990).
- [10] S.R. White, Phys. Rev. Lett. **69**, 2863 (1992), Phys. Rev. B **48**, 10345 (1993).
- [11] S.R. White, 1996 preprint, cond-mat/9604129.
- [12] F.C. Zhang, T.M. Rice, Phys. Rev. B **37**, 3759 (1988).
- [13] M. Ogata and P.W. Anderson, Phys. Rev. Lett. **70**, 3087 (1993).
- [14] R.J. Bursill , G.A. Gehring, D.J.J. Farnell, J.B. Parkinson, Chen Zeng, T. Xiang, preprint, cond-mat/9511044.
- [15] R. Chitra, S. Pati, H.R. Krishnamurthy, D. Sen, and S. Ramasesha, Phys. Rev. B **52**, 6581 (1995).

- [16] S. R. White and I. Affleck, preprint, cond-mat/9602126.
- [17] B.I. Shraiman and E.D. Siggia, Phys. Rev. Lett. **60**, 740 (1988).
- [18] A. Sandvik, D.J. Scalapino, and E. Dagotto have studied the magnetic properties of static holes in antiferromagnetic Heisenberg ladders and 2D clusters (unpublished).
- [19] M. Boninsegni and E. Manousakis, Phys. Rev. B **47**, 11897 (1993).
- [20] S.R. White, R.M. Noack, and D.J. Scalapino, Phys. Rev. Lett. **73**, 886 (1994).
- [21] M Reigrotzki, H. Tsunetsugu, and T.M. Rice, J. Phys. Cond. Matt. **6**, 9235 (1994). (1988).
- [22] G. Sierra, preprint, cond-mat/951207.
- [23] H. Tsunetsugu, M. Troyer, and T.M. Rice, Phys. Rev. B **51**, 16456 (1995).
- [24] A. Moreo and E. Dagotto, Phys. Rev. B **41**, 9488 (1990).
- [25] D.J. Scalapino and S.A. Trugman, to appear in Philosophical Mag.
- [26] V.J. Emery, S.A. Kivelson, and H.Q. Lin, Phys. Rev. Lett. **64**, 475 (1990) and Phys. Rev. B **42**, 6523 (1990).
- [27] V.J. Emery and S.A. Kivelson, Physica C **207**, 597 (1993).

FIGURES

FIG. 1. Spin structure near a single hole (the gray circle) on a 1D t - J lattice. (a) Néel spin configuration, shifted by one spacing to the right of the hole. (b,c) Valence bond configurations with a hole. (d,e) Results of a DMRG calculation for the ground state of a 15 site t - J system, with $J/t = 0.5$, and open boundary conditions. The thickness of the lines is proportional to the bond strengths, $\langle \psi | \vec{S}_i \cdot \vec{S}_j P_h(h) | \psi \rangle / \langle \psi | P_h(h) | \psi \rangle$, according to the scale shown. In (d), $h = 7$, and in (e), $h = 8$. (f) Results of a DMRG calculation for the ground state of a 16 site system, with $J/t = 0.5$, and open boundary conditions. The length of the arrow is proportional to $\langle S^z P_h(h) \rangle / \langle \psi | P_h(h) | \psi \rangle$.

FIG. 2. A single hole on a two-chain ladder. Gray circles are dynamic holes, and black circles are static vacancies. Pictured is the central region of a 32×2 lattice, with open boundary conditions. All results are for $J/t = 0.5$. (a) The bond strengths $\langle \vec{S}_i \cdot \vec{S}_j \rangle$ about a dynamic hole, as in Fig. 1(d)-(e). All nearest-neighbor bonds are shown. In addition, if two sites are both adjacent to the hole, and if the bond is antiferromagnetic, $\langle \vec{S}_i \cdot \vec{S}_j \rangle < 0$, it is also shown. (b) $\langle S^z \rangle$, as in Fig. 1(f). (c) The bond strengths $\langle \vec{S}_i \cdot \vec{S}_j \rangle$ about a static vacancy. (d) $\langle S^z \rangle$ about a static vacancy.

FIG. 3. Two dynamic holes (gray circles) on a two-chain ladder. Pictured is the central region of a 32×2 lattice, with open boundary conditions. (a) The hopping energy $-t \sum_s \langle c_{i,s}^\dagger c_{j,s} + c_{j,s}^\dagger c_{i,s} \rangle$ for each link when one hole is projected onto a particular site. The hopping energy shown is associated with the hole which has not been projected onto a particular site. The thickness of the lines is proportional to energy, according to the scale shown. (b-d) The bond strengths $\langle \vec{S}_i \cdot \vec{S}_j \rangle$ after both holes have been projected. Next-nearest-neighbor bonds are shown if i and j are both adjacent to the same hole, and if the bond is antiferromagnetic.

FIG. 4. Dynamic holes on a three-chain ladder, plotted similarly to Figs. 2 and 3. Parts (a)-(e) are for a single hole, and (f) is for two holes. Pictured is the central region of a 16×3 lattice, with open boundary conditions. (a) The hopping energy for each link. (b,c) The bond strengths $\langle \vec{S}_i \cdot \vec{S}_j \rangle$. (d,e) $\langle S^z \rangle$ for each site about the hole. (f) The hopping energy in a two-hole system when one hole has been projected onto one of its most probable locations.

FIG. 5. A single dynamic hole on a four-chain ladder. All calculations are on a 16×4 lattice, with open boundary conditions. Only the central region is shown. (a,b) The bond strengths $\langle \vec{S}_i \cdot \vec{S}_j \rangle$ for two different hole locations. (c,d) The difference in bond strengths $\langle \vec{S}_i \cdot \vec{S}_j \rangle$ between the system with the dynamic hole [as in (a) and (b)] and the same bond on the equivalent *undoped* system. Solid lines indicate stronger bonds, and dashed indicate weaker. Next-nearest-neighbor bonds are not shown. (e,f) The difference in bond strengths between the system with a *static* hole or vacancy (black circle) and the equivalent undoped system.

FIG. 6. Two dynamic holes on a four-chain ladder. The figure shows the hopping energy of one dynamic hole when the other has been projected onto a particular site. All calculations are on a 16×4 lattice, with open boundary conditions. Only the central region is shown.

FIG. 7. Exchange energy for a 16×4 system, with open boundary conditions, and two dynamic holes.

FIG. 8. A single dynamic hole on a five-chain ladder. All calculations are for an 8×5 lattice, with open boundary conditions. (a) The hopping energy of the hole. (b) The bond strengths about the hole. (c) $\langle S^z \rangle$ for each site about the hole.

FIG. 9. Two dynamic holes on a five-chain ladder. (a) The hopping energy for an 8×5 cluster, with open boundary conditions. (b) The hopping energy for the system shown in (a) with one hole projected onto a site. (c) The hopping energy for an 10×5 cluster, with open boundary conditions. (d) The hopping energy for the system shown in (c) with one hole projected onto a site.

FIG. 10. A single dynamic hole on a 8×6 system, with open boundary conditions. (a) The hopping energy of the hole. (b) The bond strengths about the hole. (c) The difference in bond strengths between the system with the dynamic hole and the same bond on the equivalent undoped system. Solid lines indicate stronger bonds, and dashed indicate weaker. (d) The difference in bond strengths between the system with a *static* hole or vacancy (black circle) and the equivalent undoped system.

FIG. 11. Two dynamic holes on a 8×6 system, with open boundary conditions. (a) The hopping energy for each link when one hole is projected onto a particular site. (b-d) The bond strengths about the pair of holes. (e,f) The difference in bond strengths between the system with the dynamic hole and the same bond on the equivalent undoped system.

FIG. 12. The 2×2 t - J cluster. Edge nearest-neighbor singlets can form as well as diagonal (1-3,2-4) next-nearest-neighbor singlets.

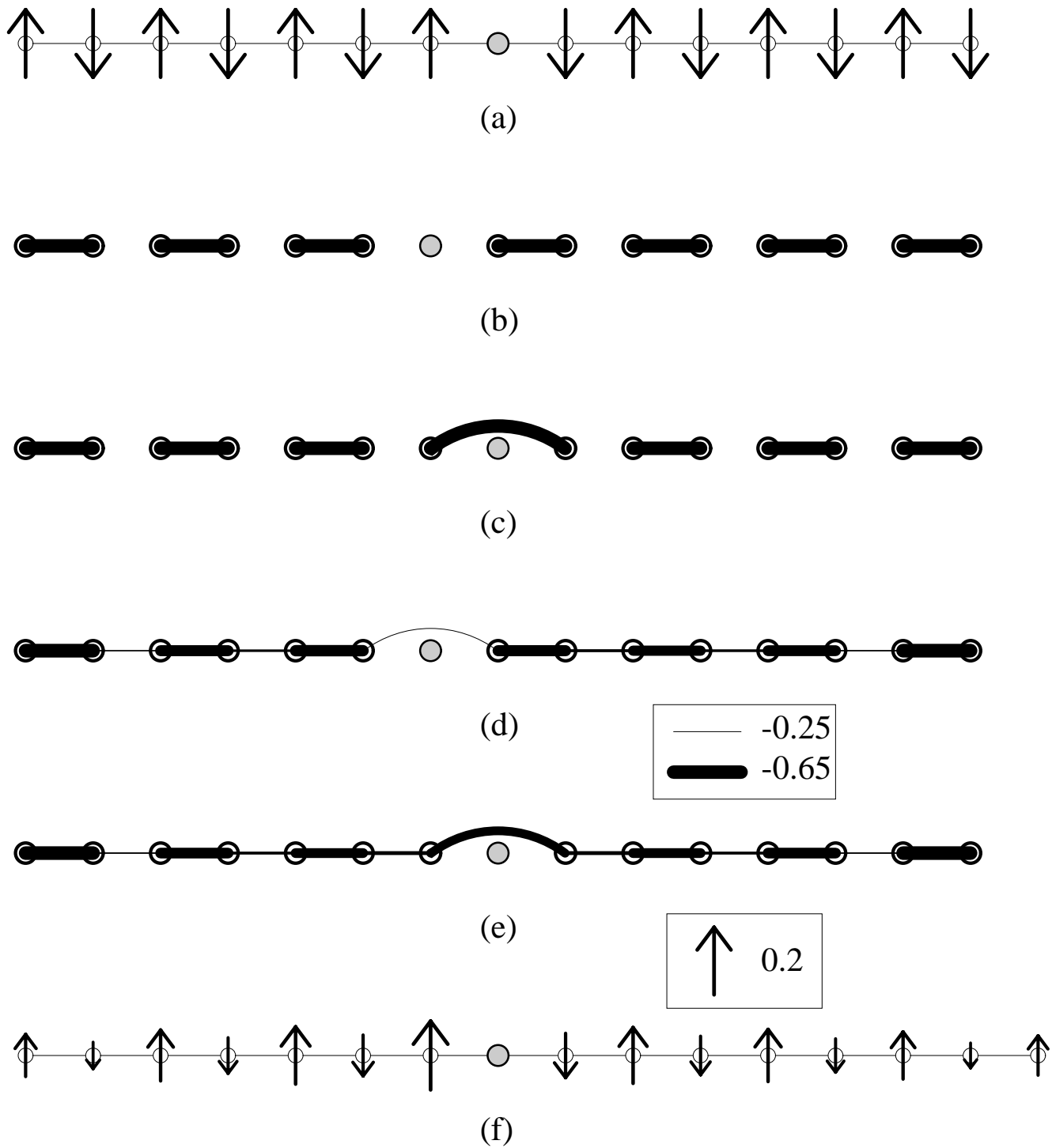


Fig. 1
White and Scalapino

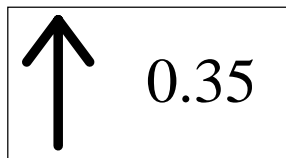
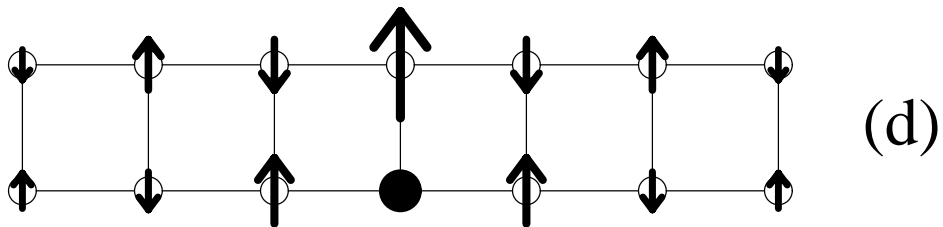
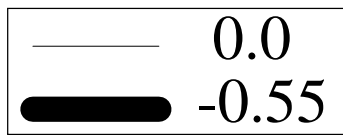
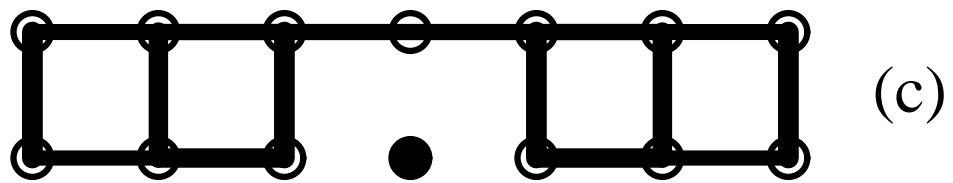
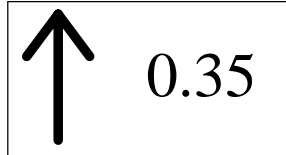
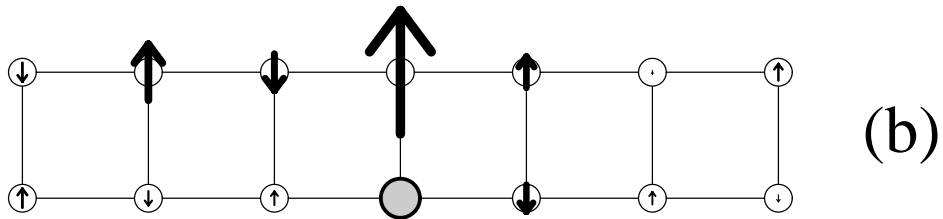
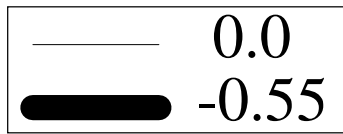
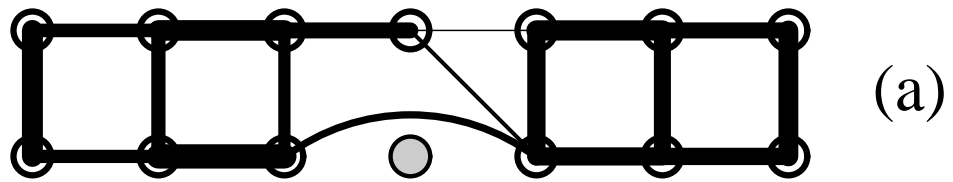


Fig. 2
 White and Scalapino

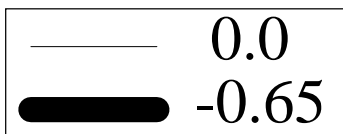
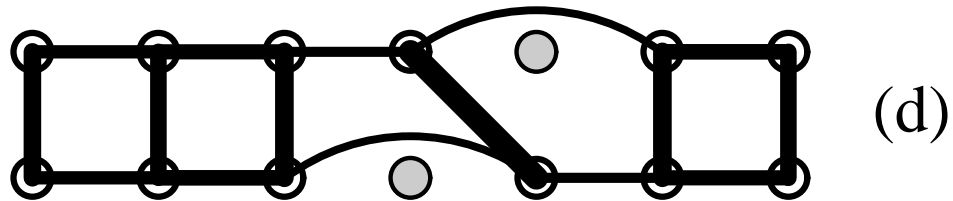
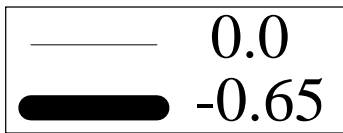
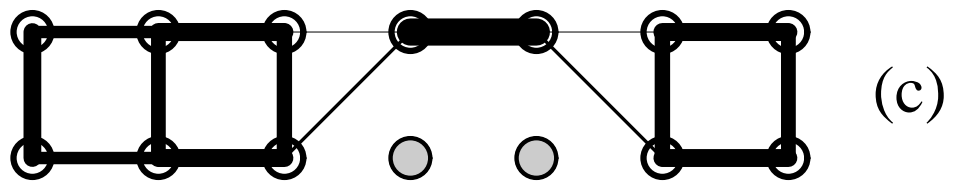
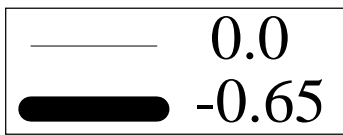
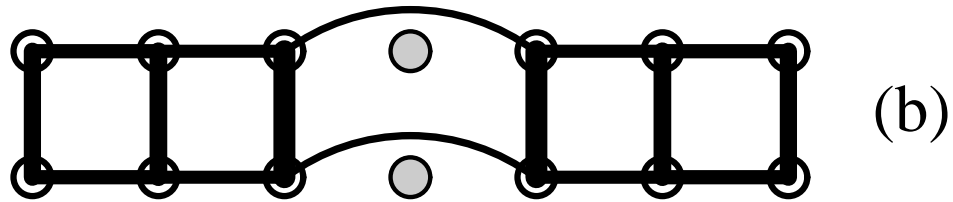
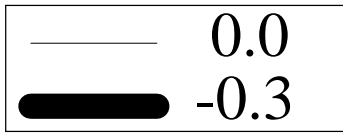
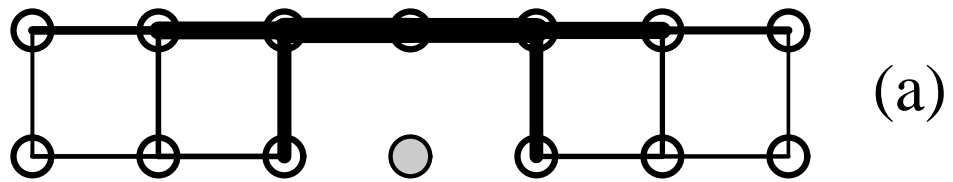


Fig. 3
 White and Scalapino

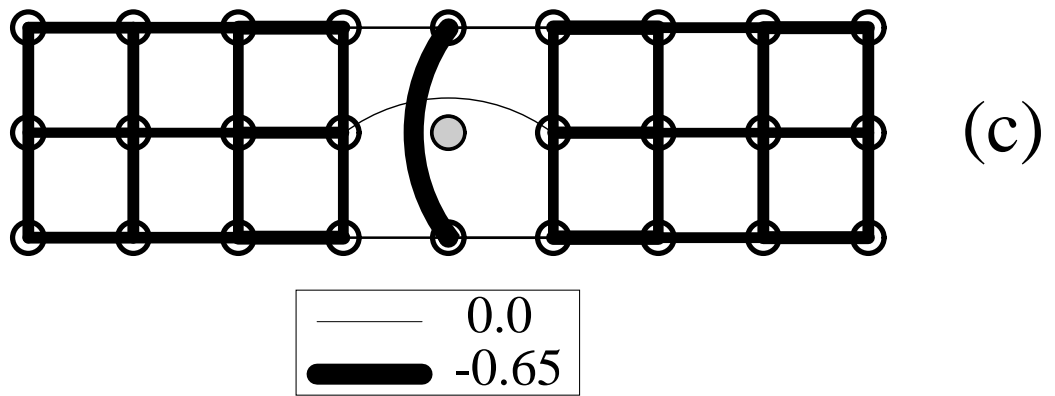
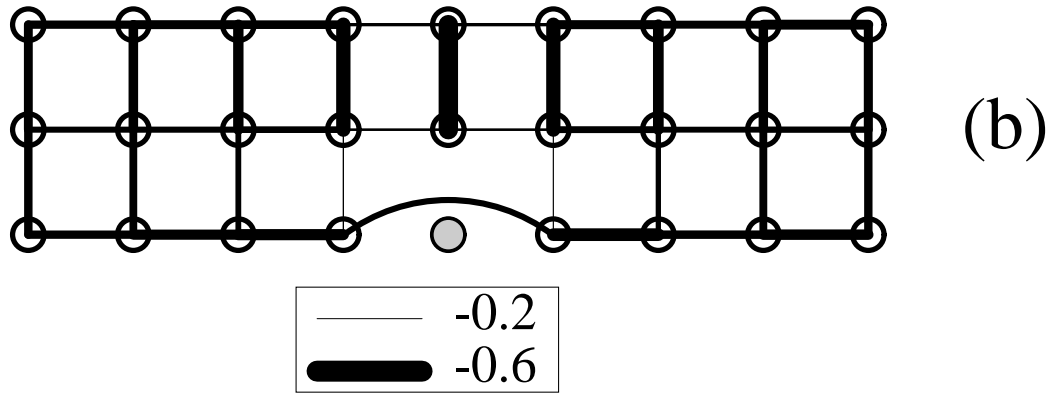
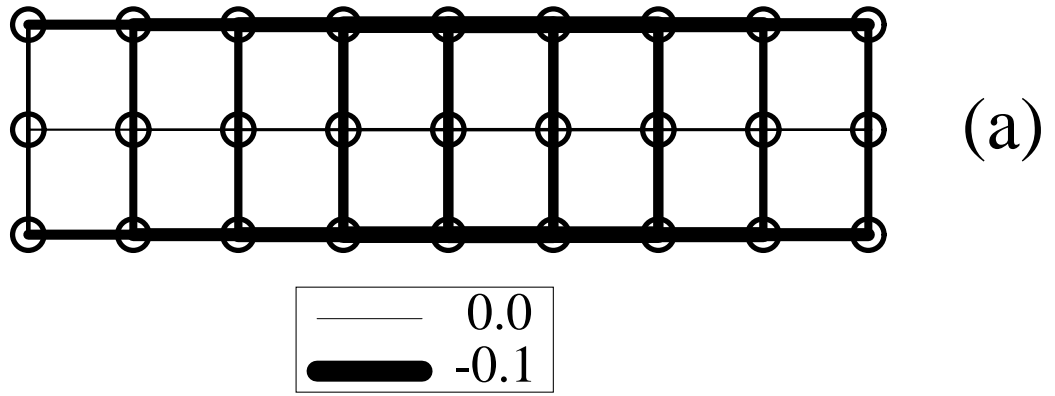


Fig. 4(a)-(c)
White and Scalapino

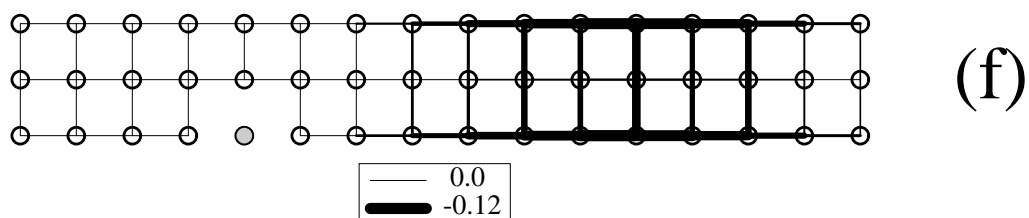
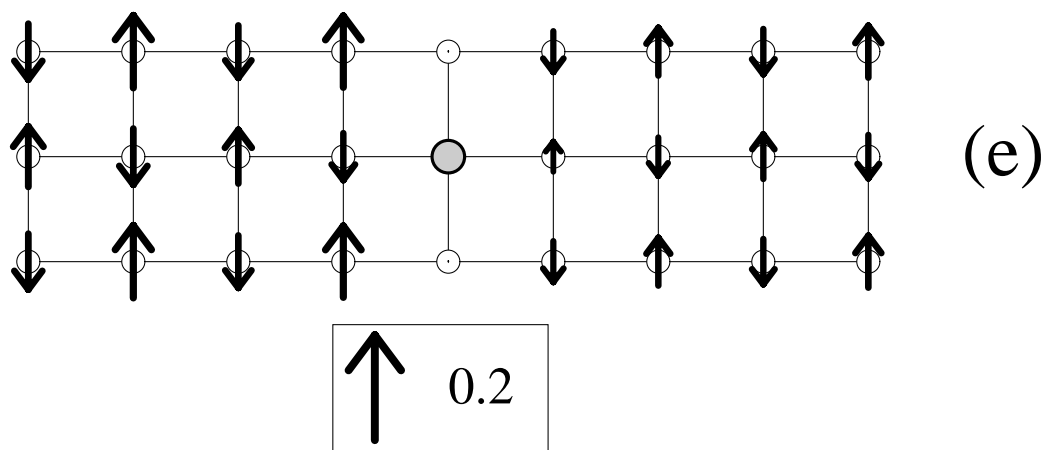
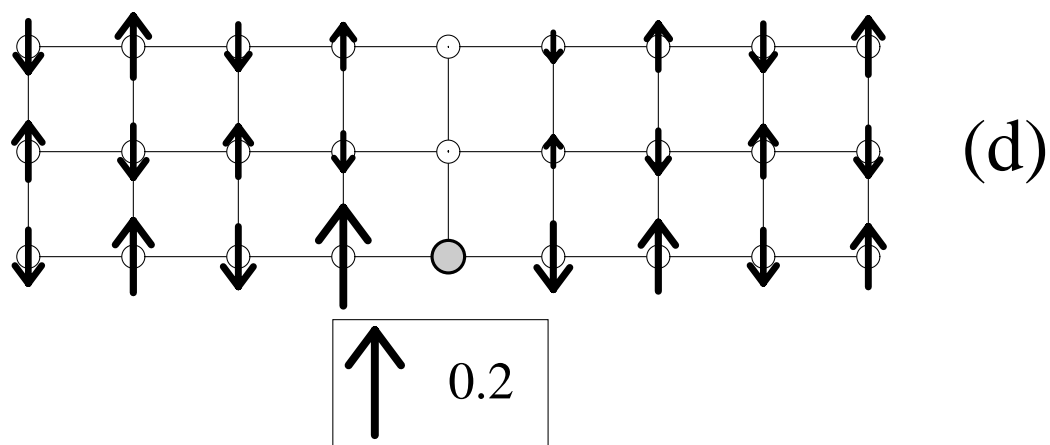


Fig. 4(d)-(f)
White and Scalapino

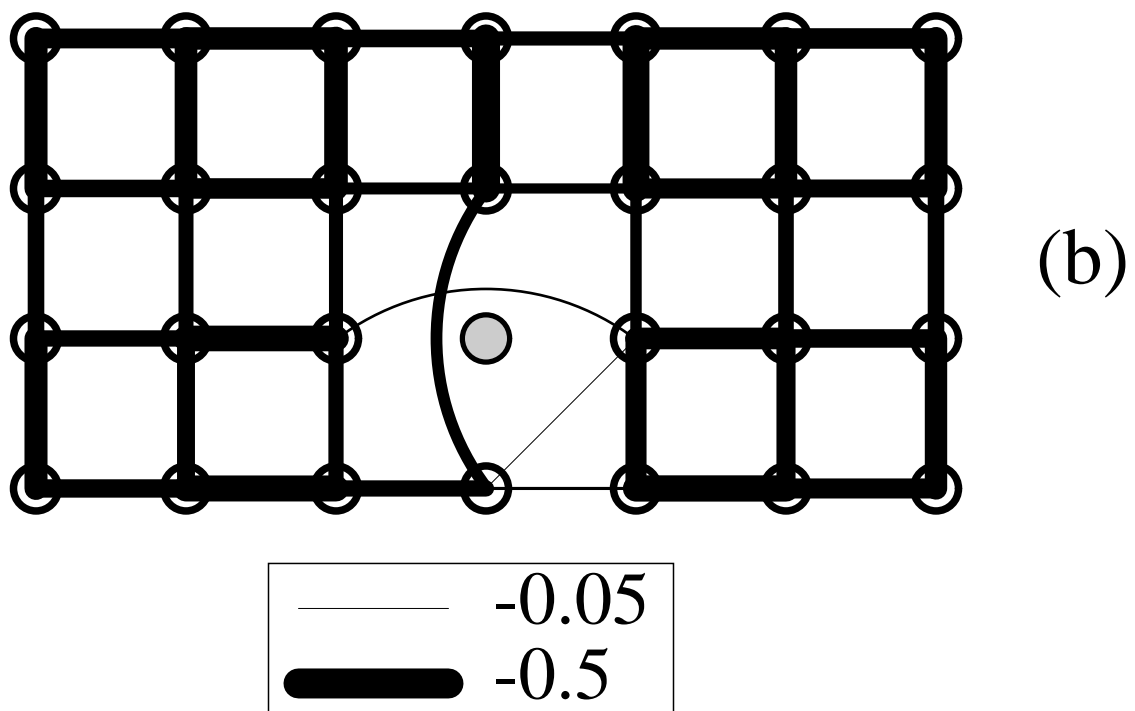
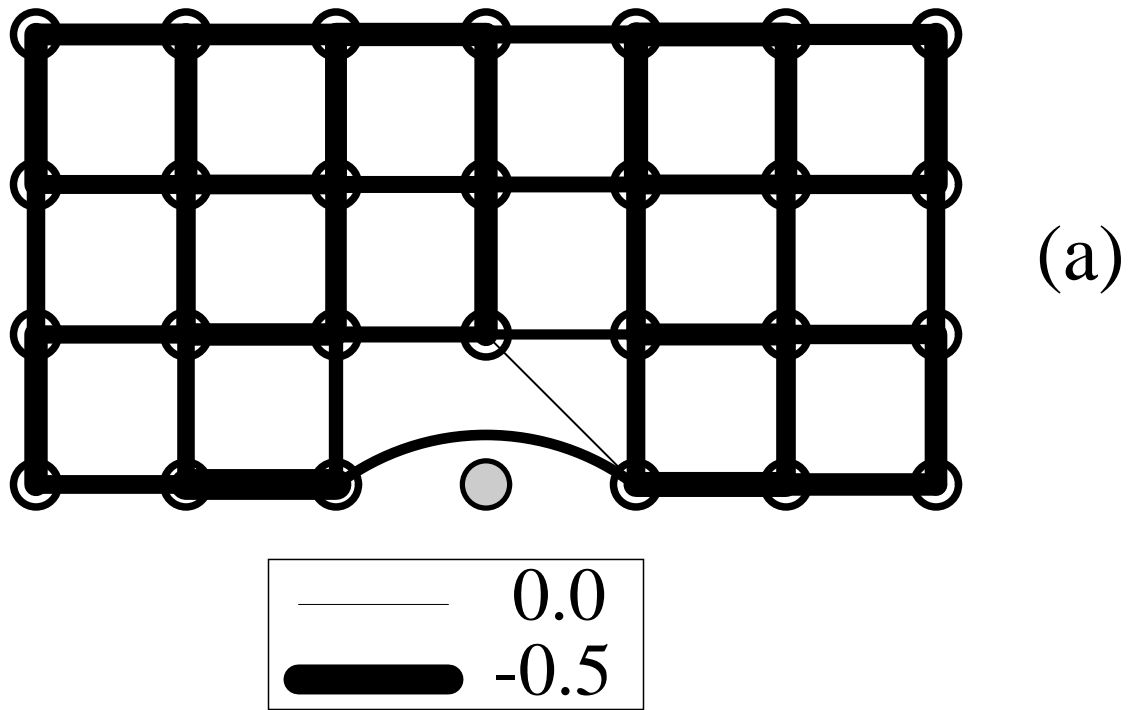


Fig. 5(a,b)
White and Scalapino

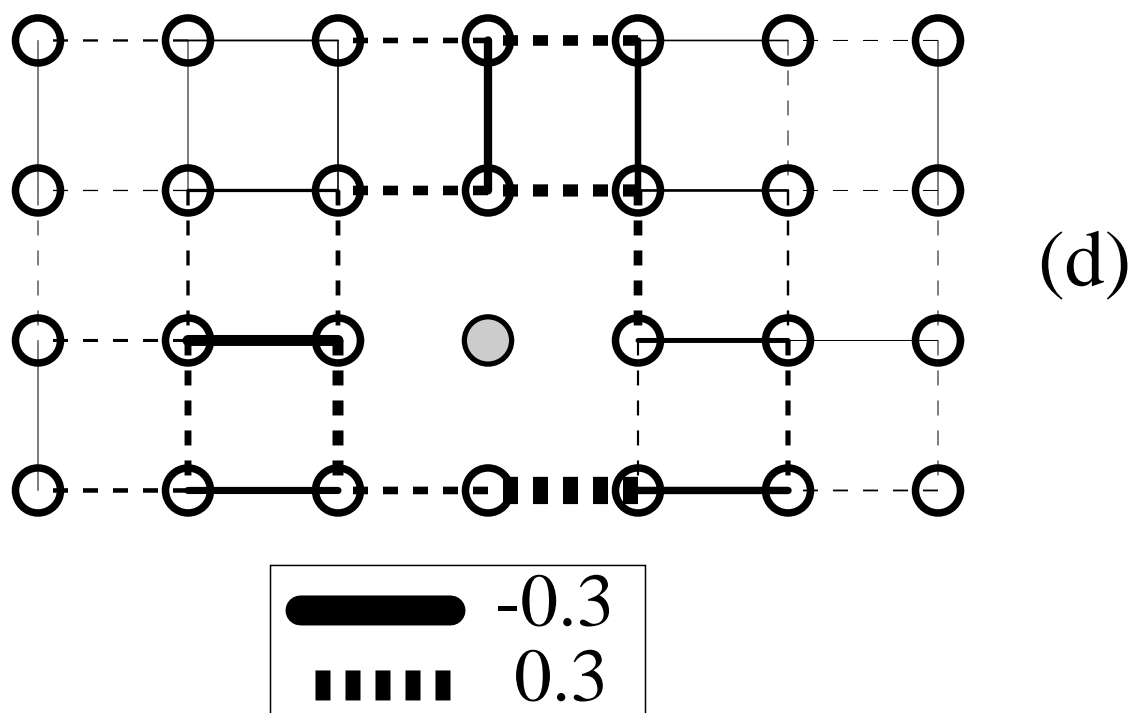
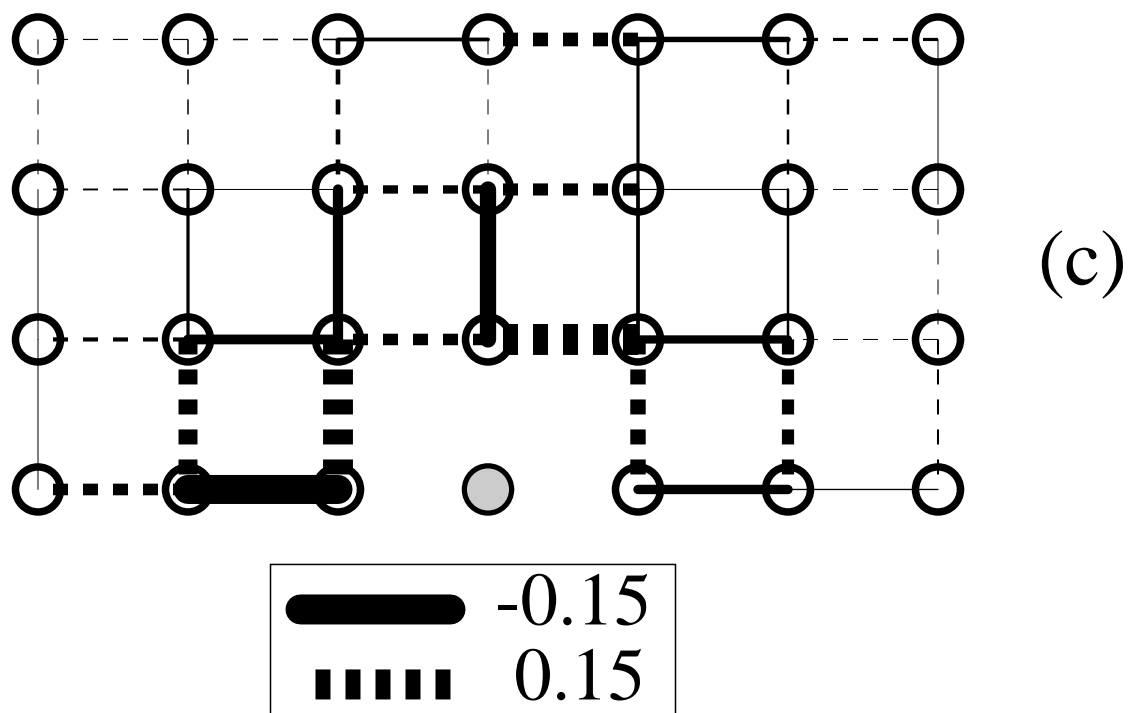


Fig. 5(c,d)
White and Scalapino

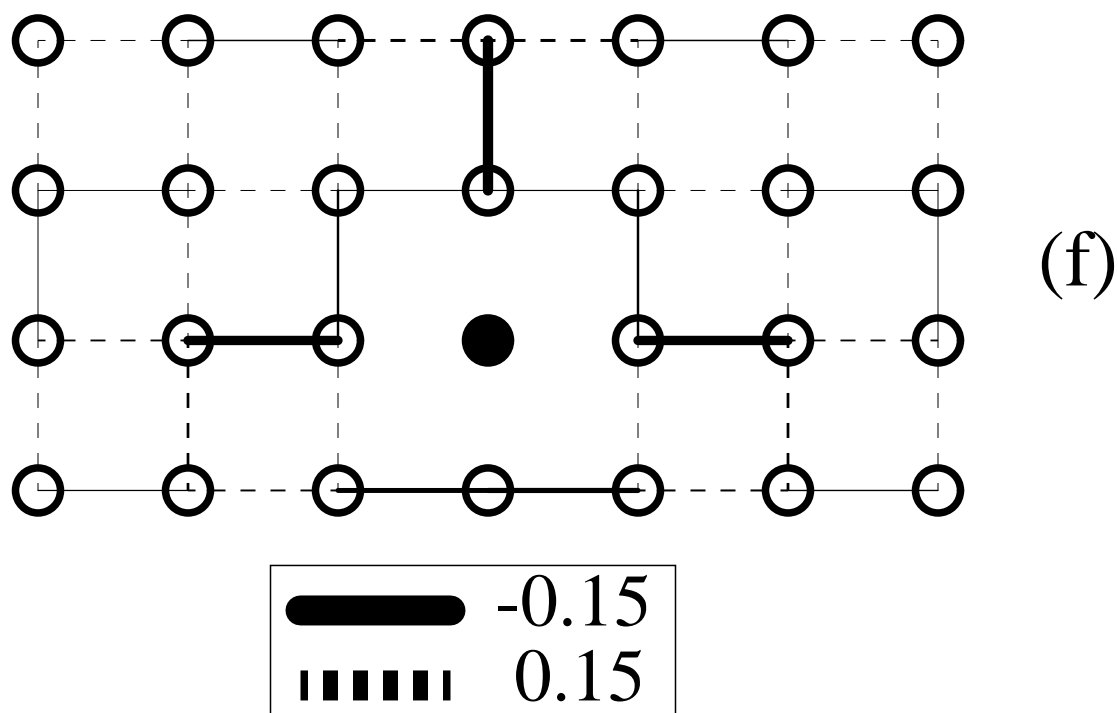
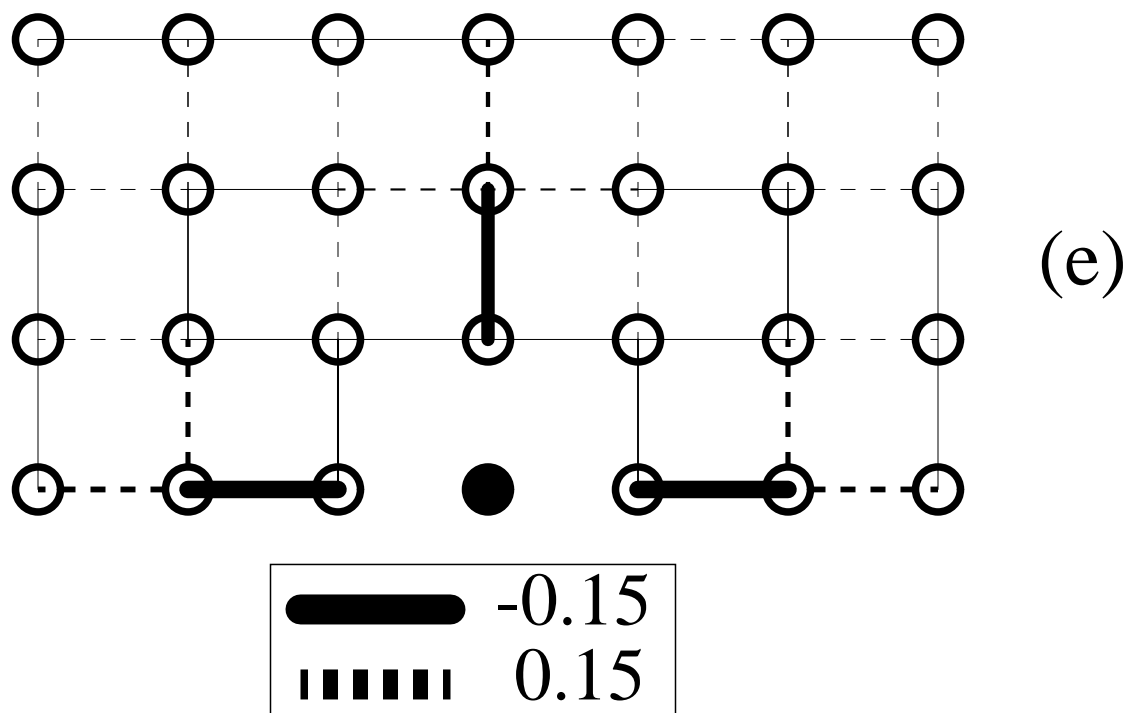


Fig. 5(e,f)
White and Scalapino

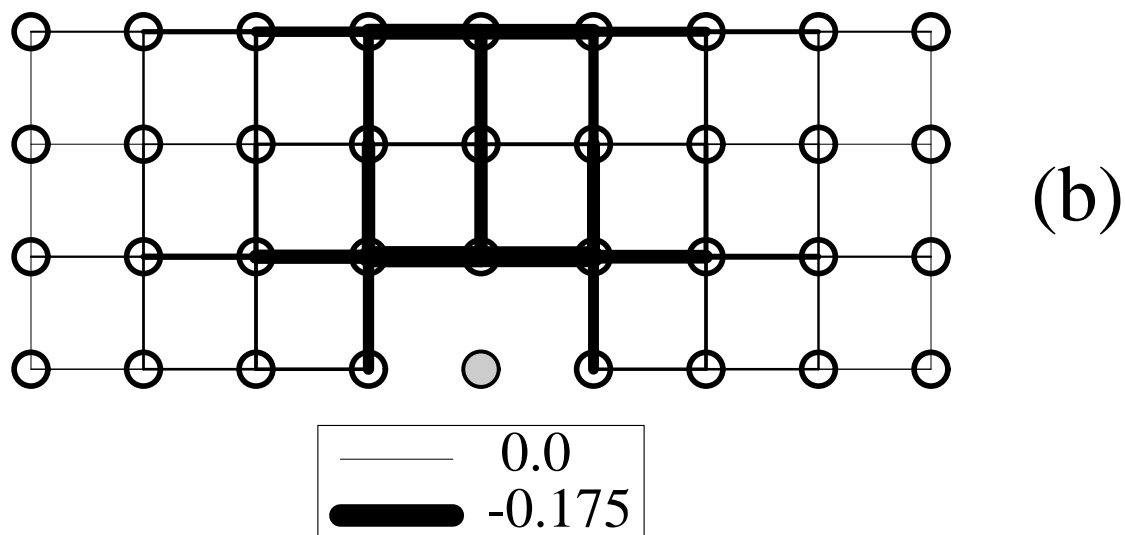
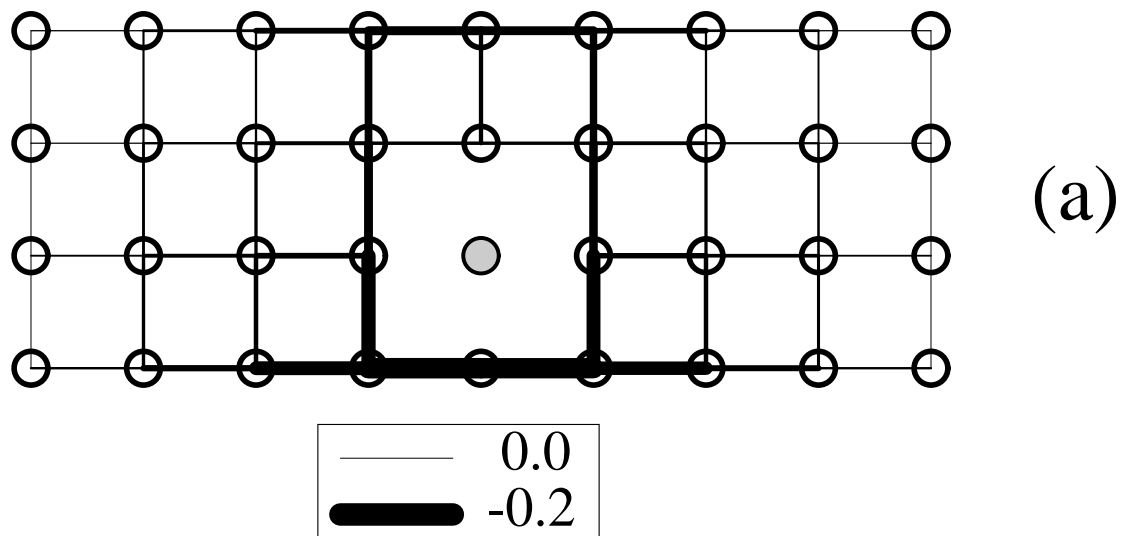


Fig. 6
White and Scalapino

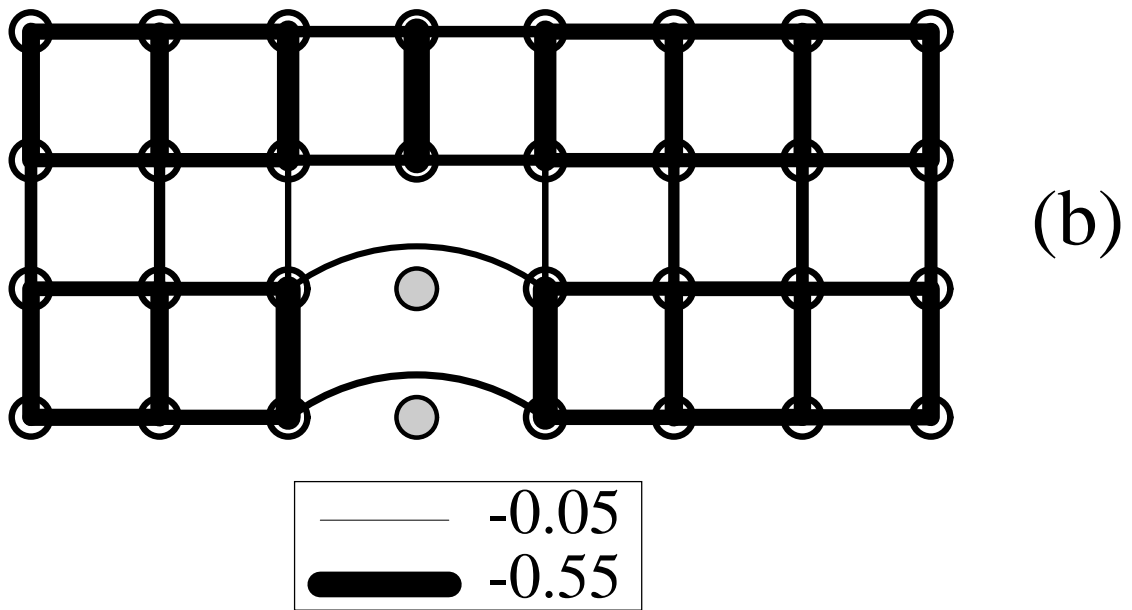
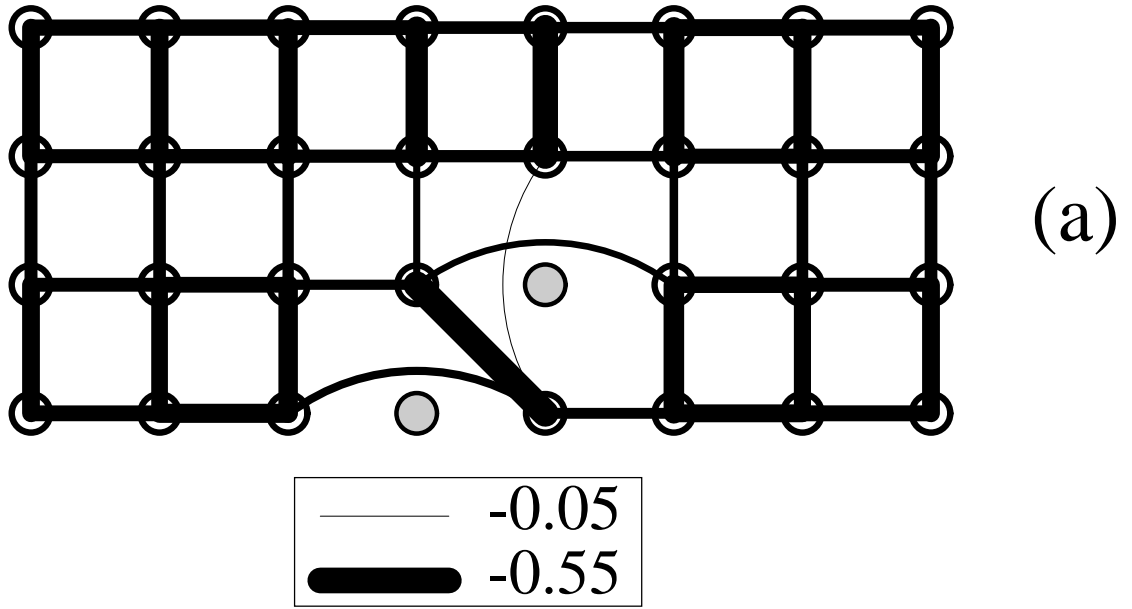


Fig. 7
White and Scalapino

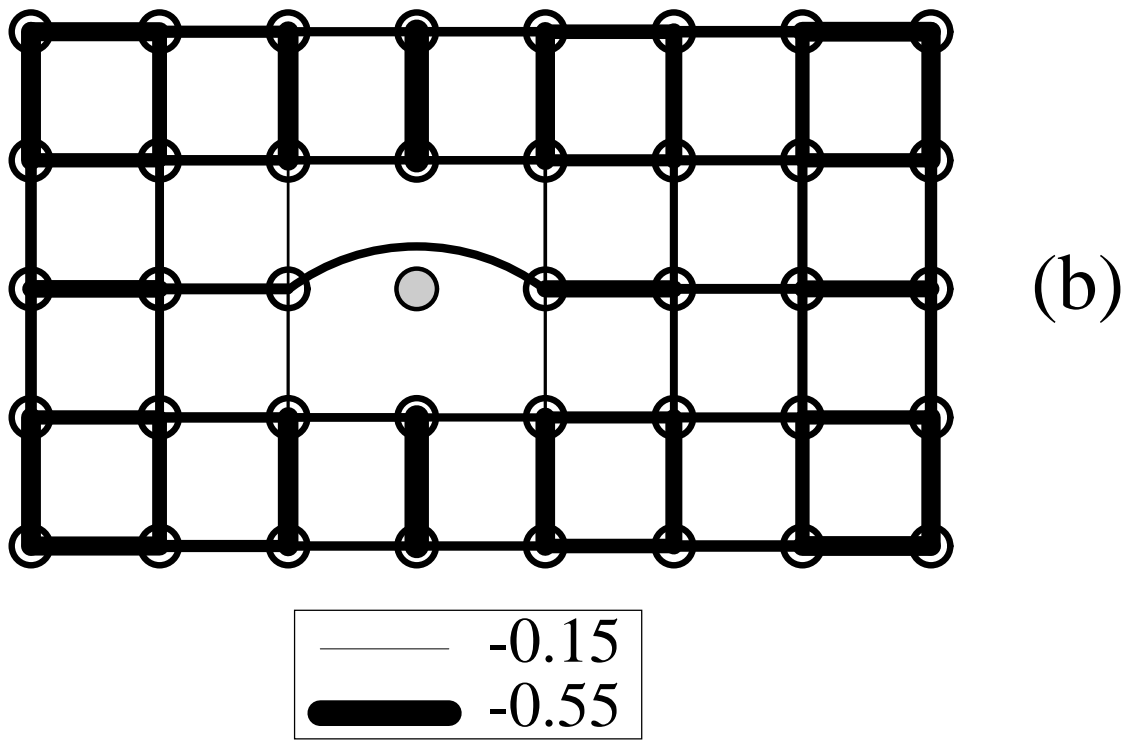
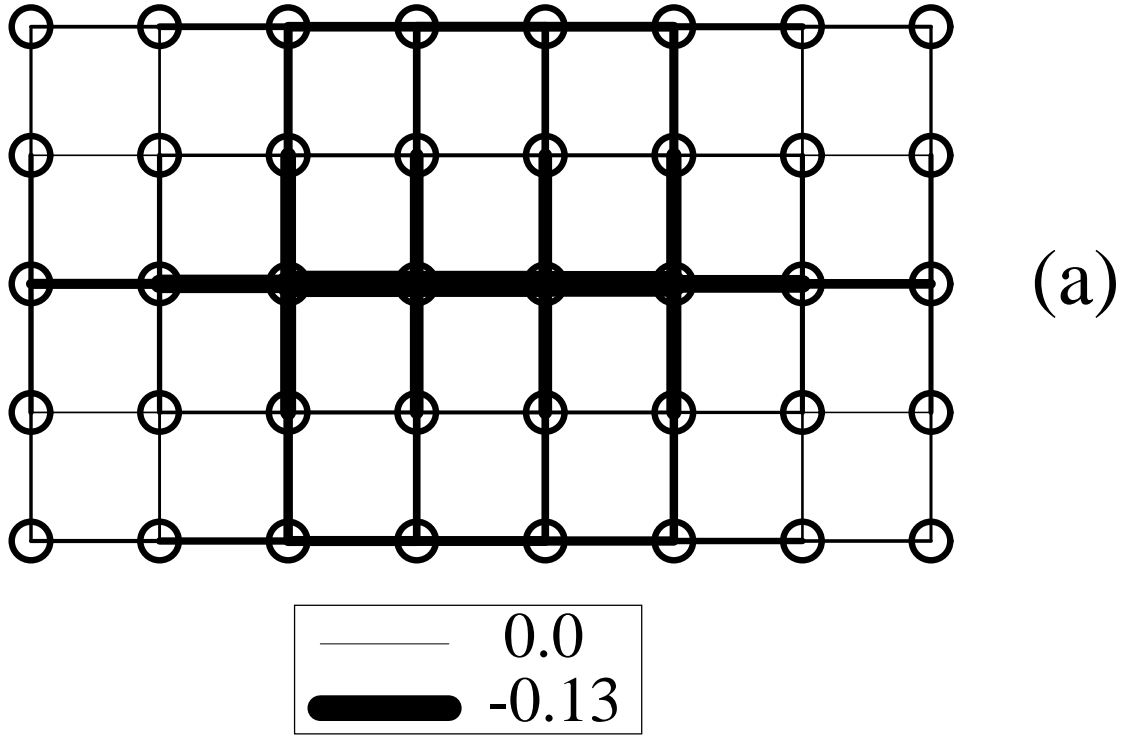


Fig. 8(a,b)
 White and Scalapino

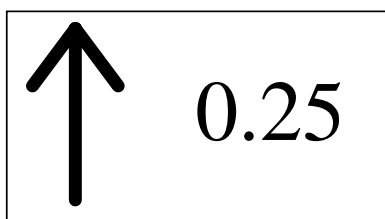
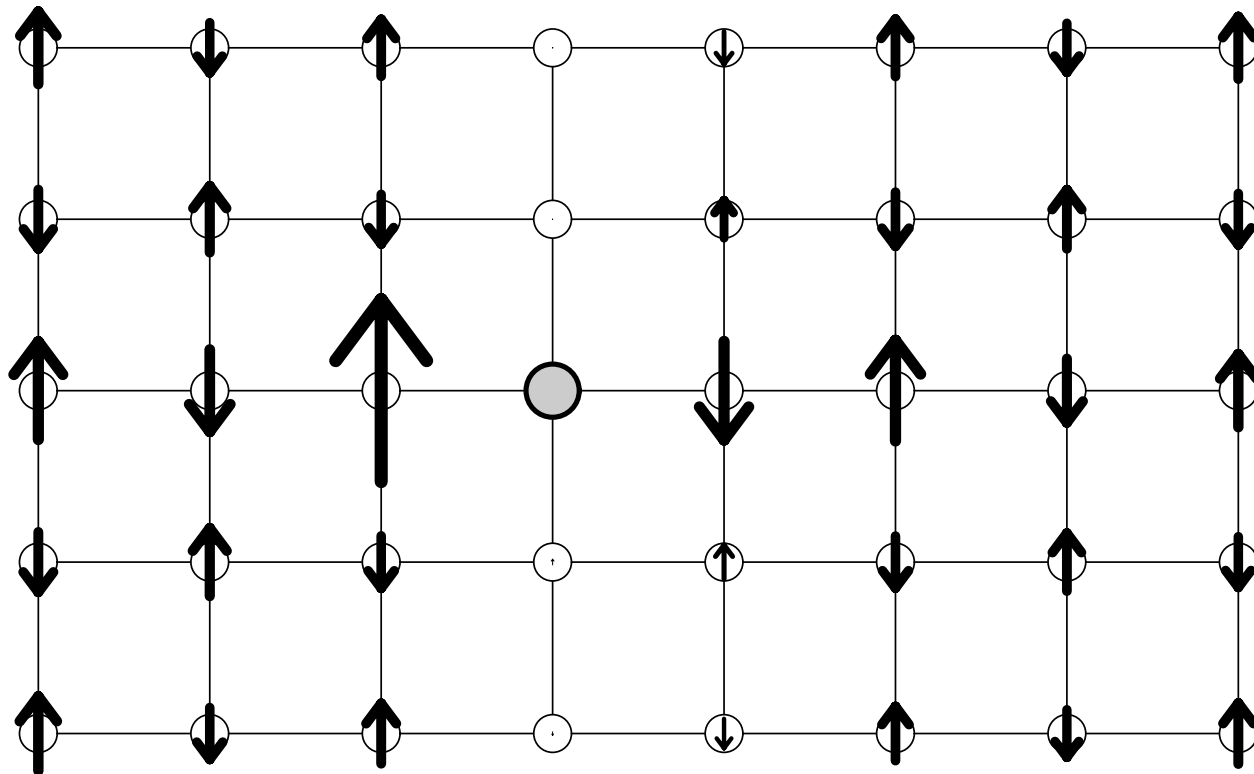


Fig. 8(c)

White and Scalapino

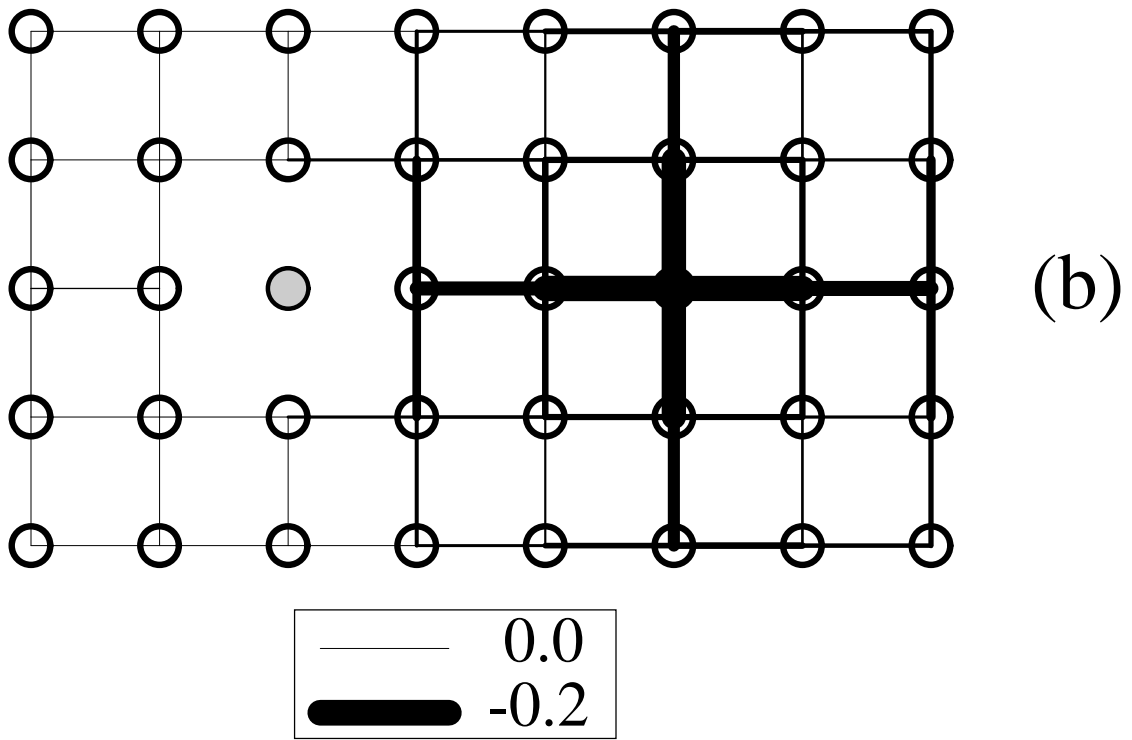
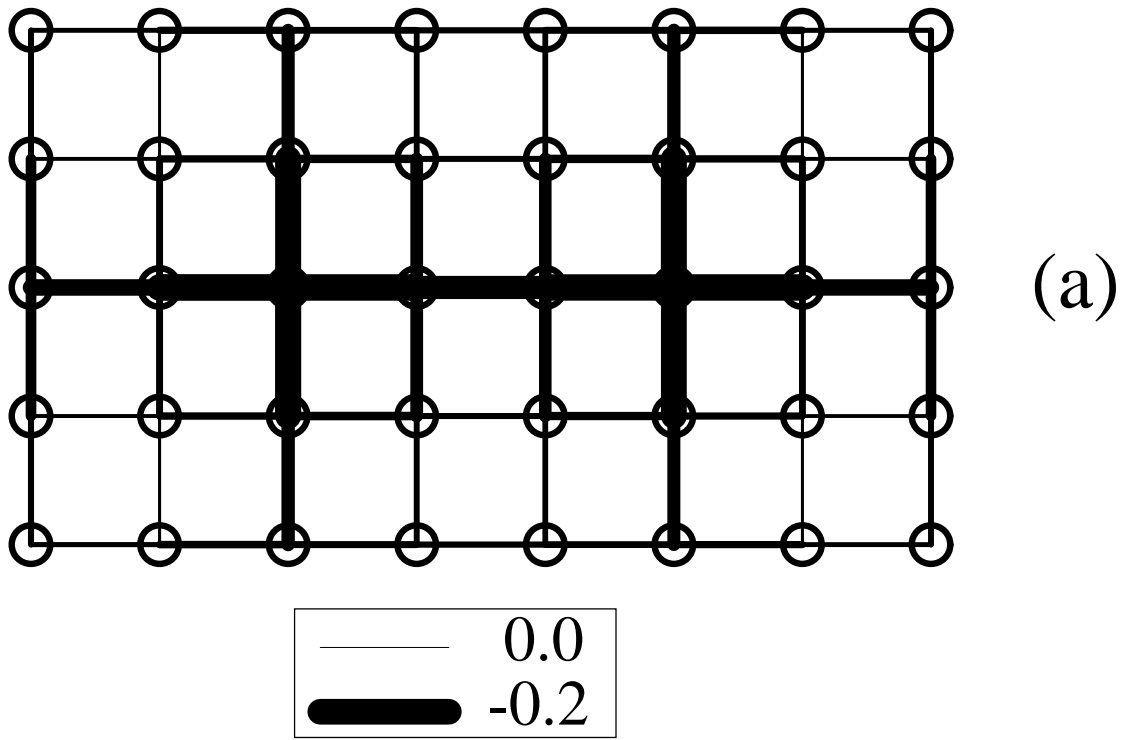


Fig. 9(a,b)
White and Scalapino

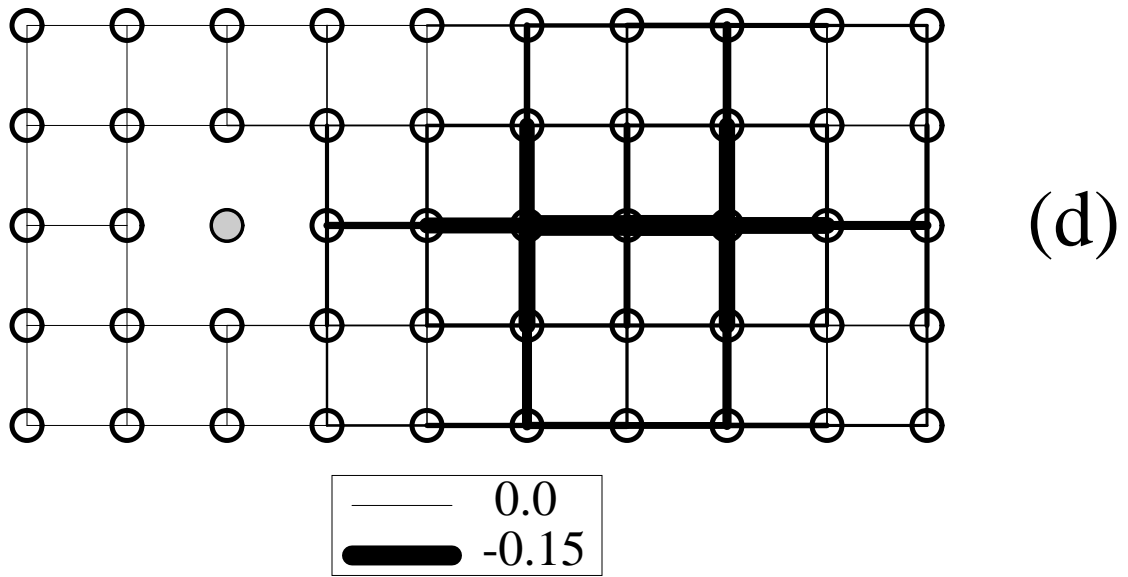
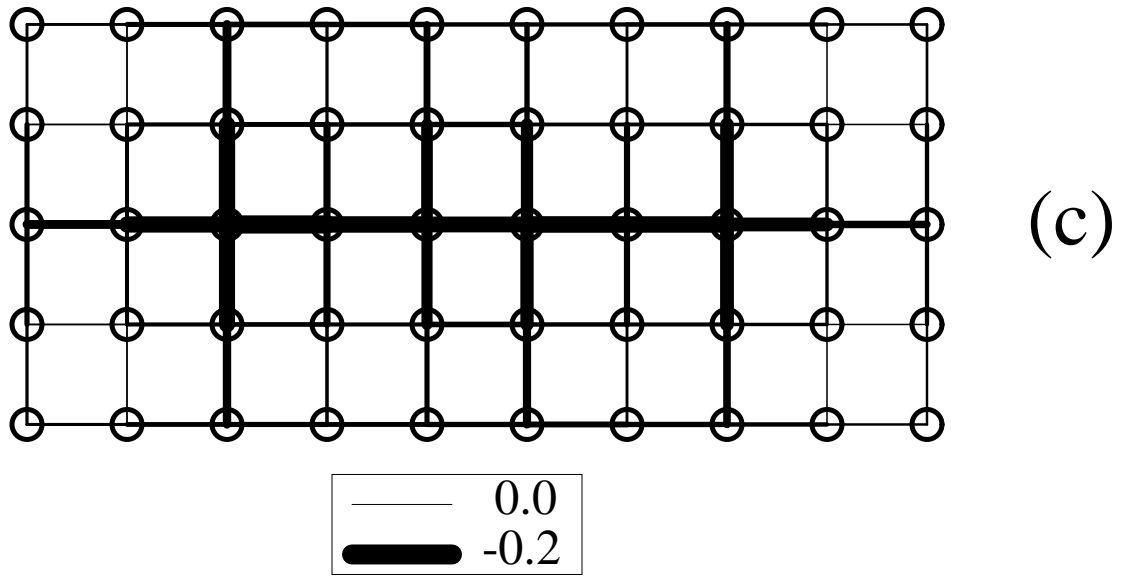


Fig. 9(c,d)
White and Scalapino

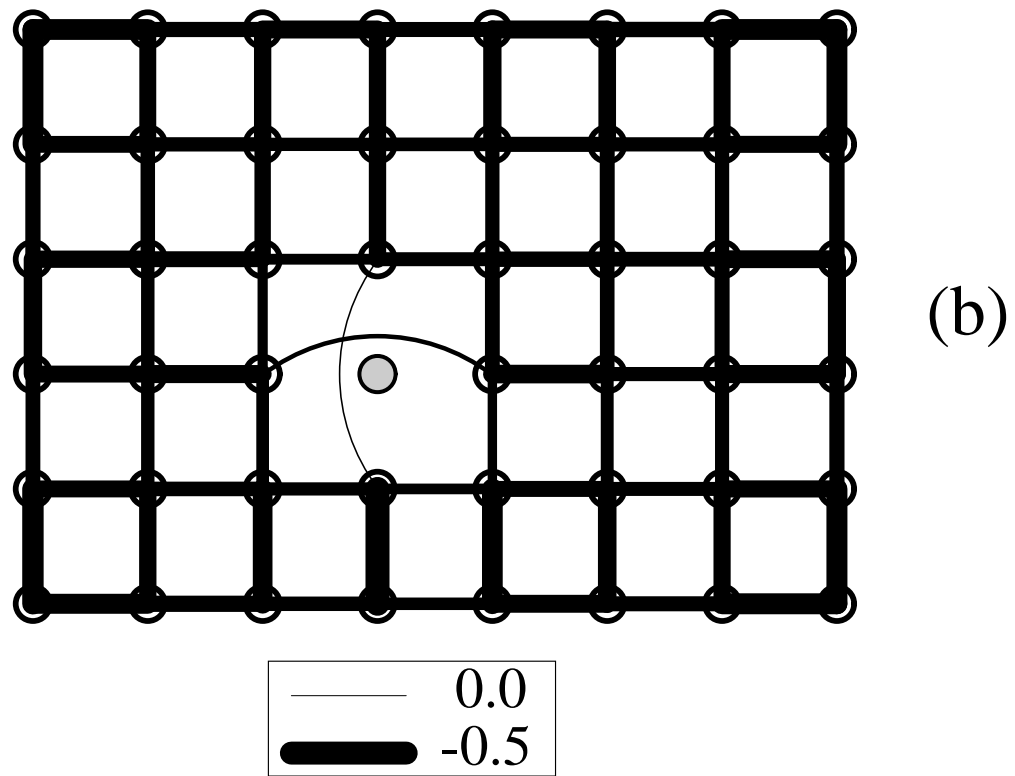
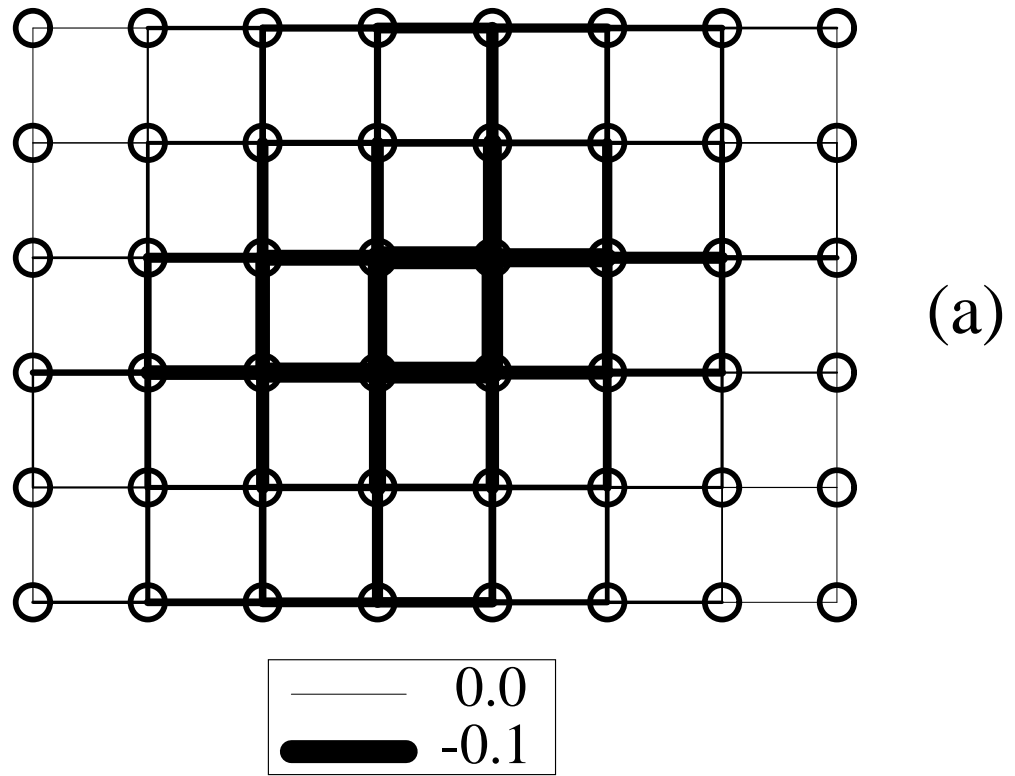


Fig. 10(a,b)
White and Scalapino

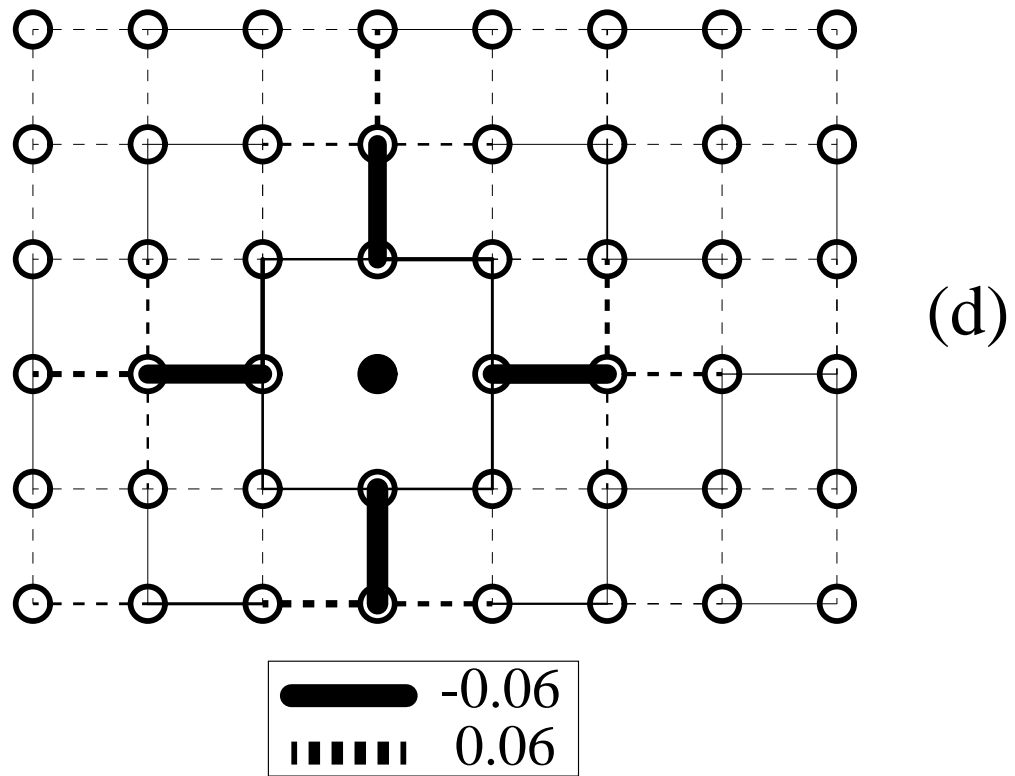
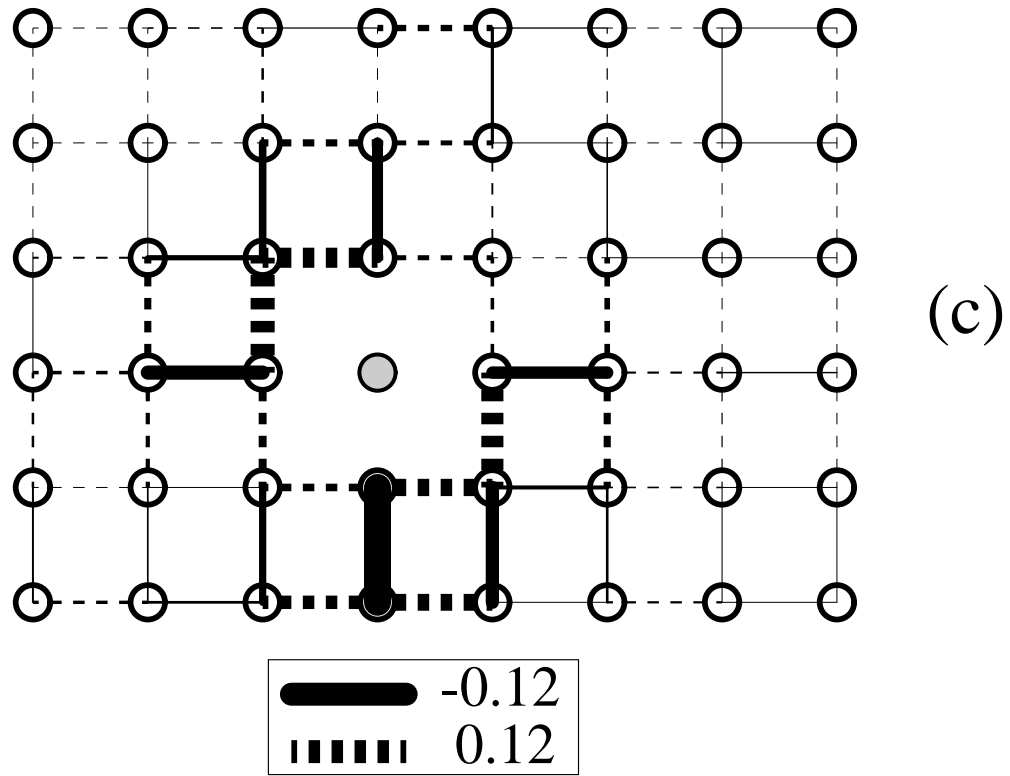


Fig. 10(c,d)
White and Scalapino

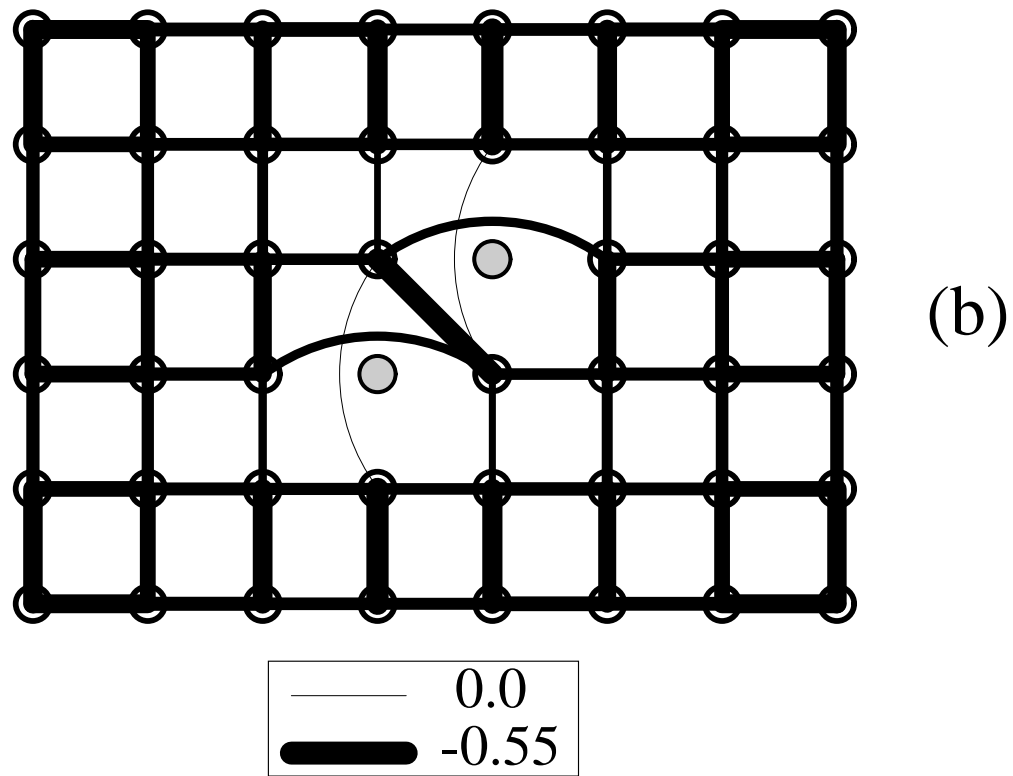
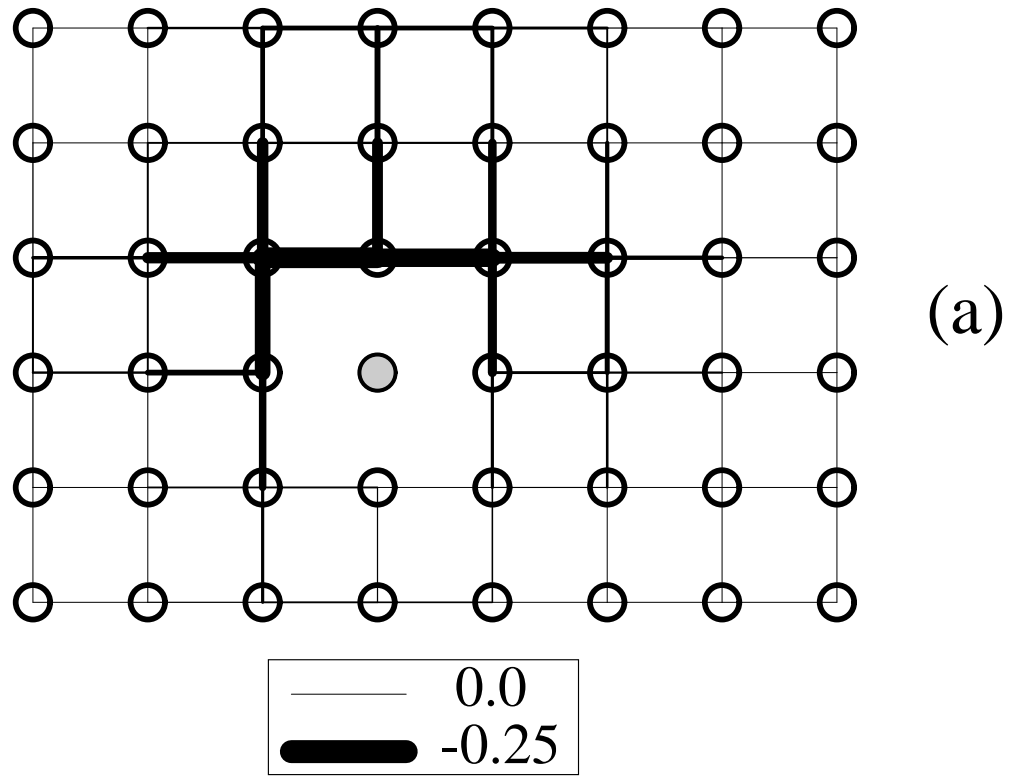


Fig. 11(a,b)
 White and Scalapino

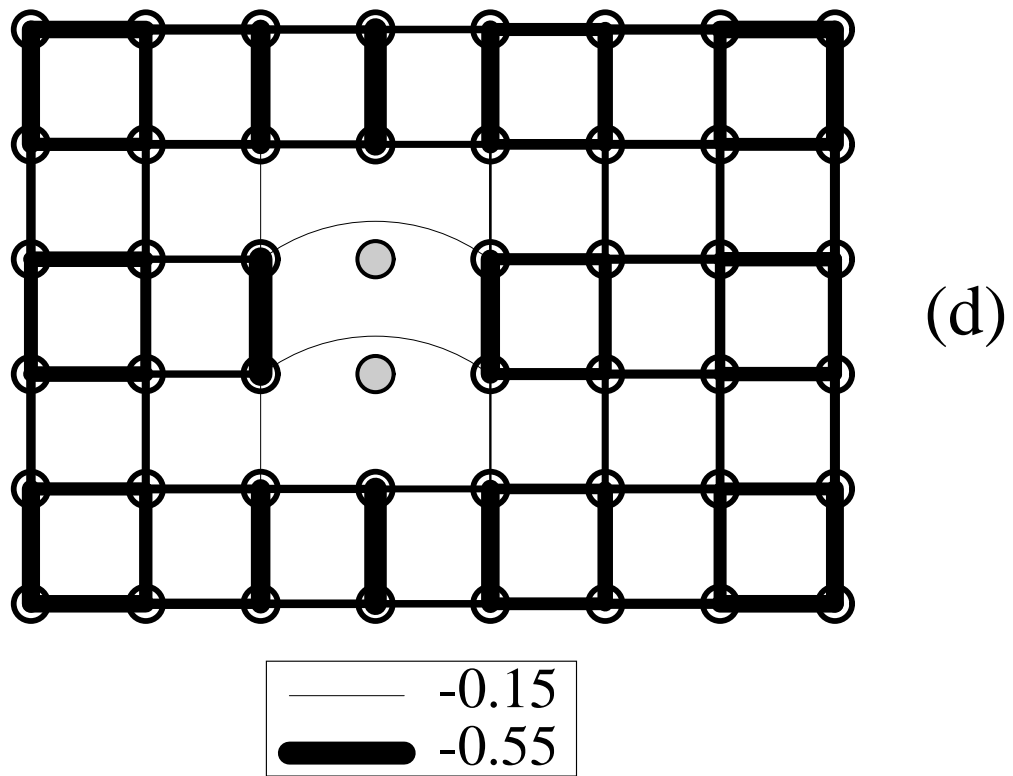
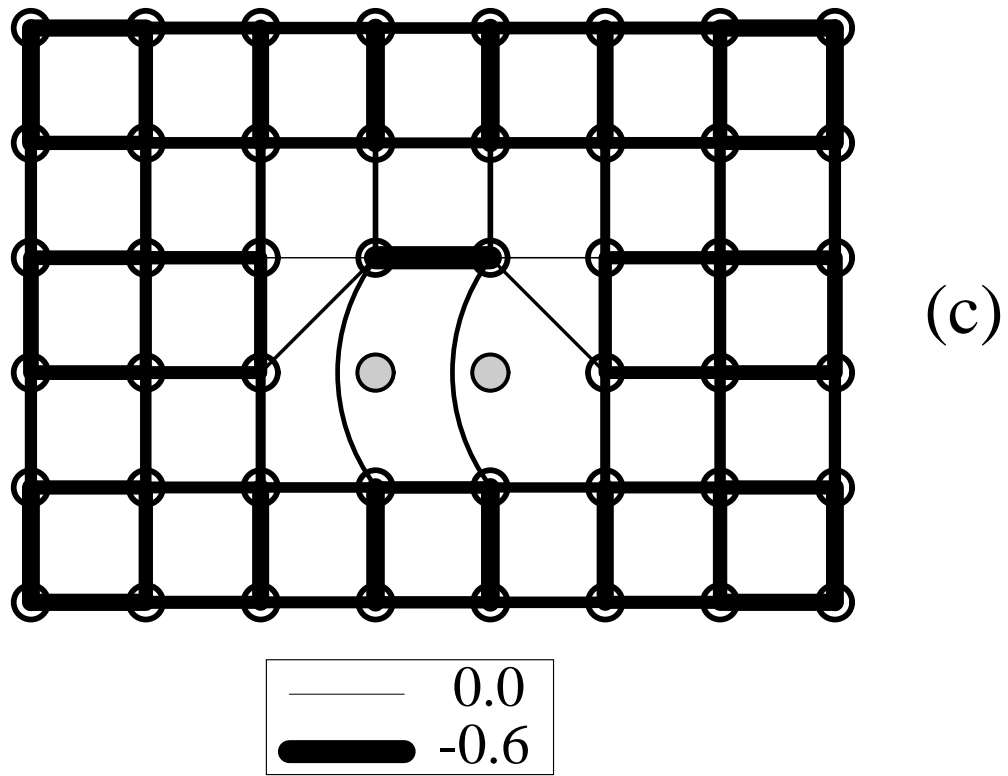


Fig. 11(c,d)
White and Scalapino

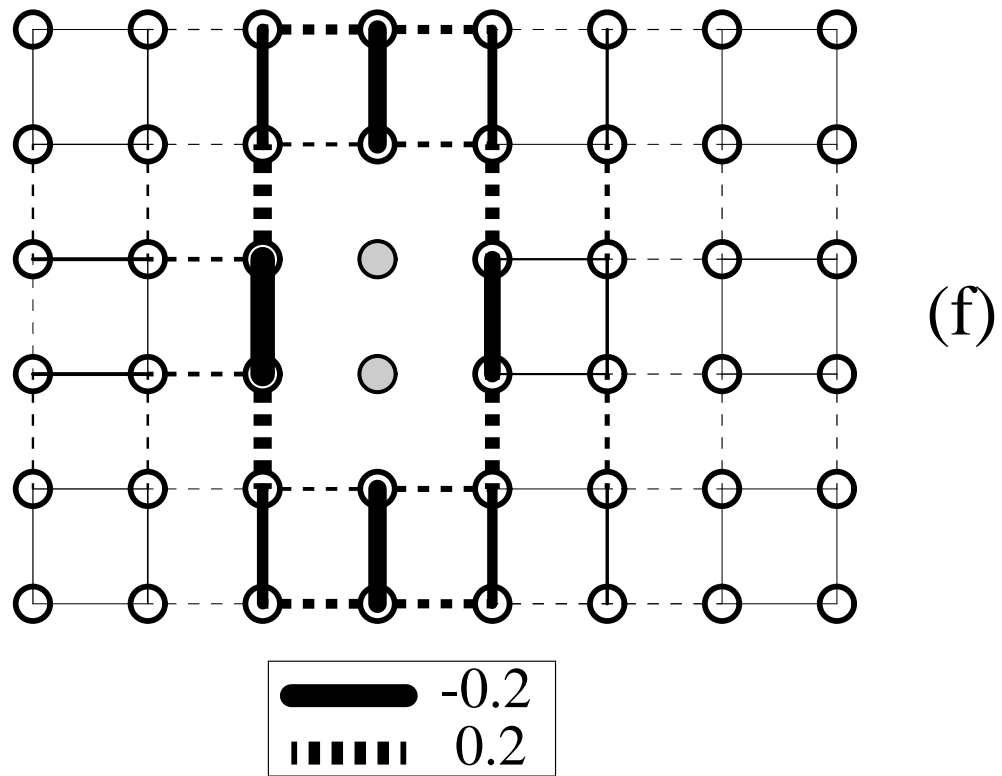
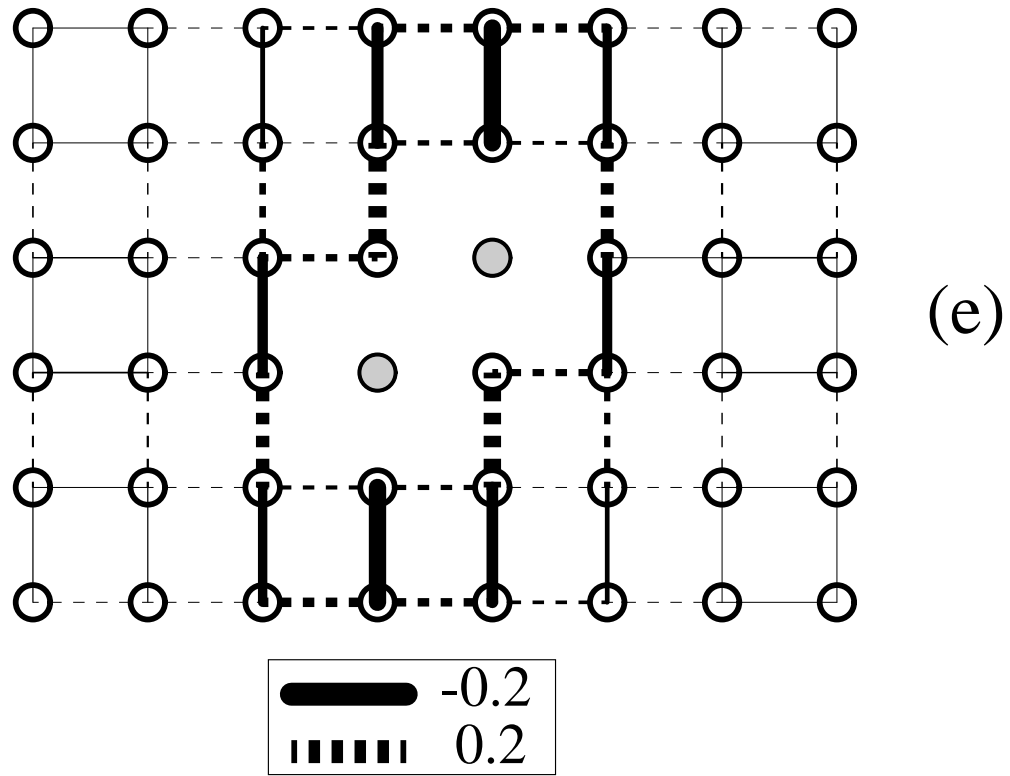


Fig. 11(e,f)
White and Scalapino

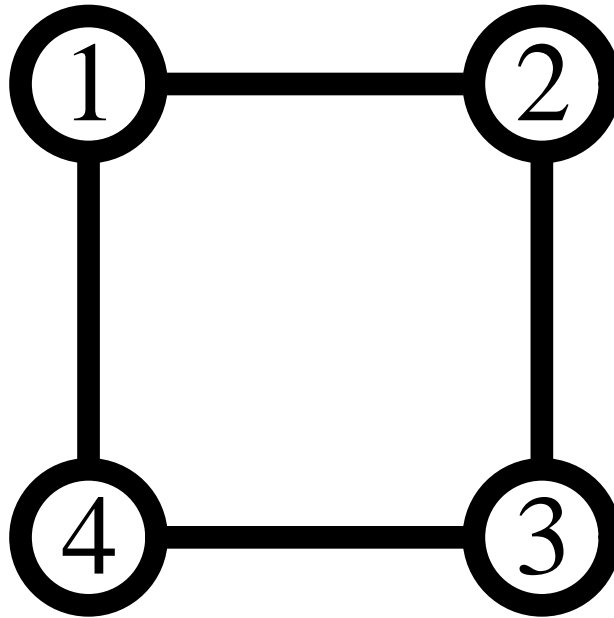


Fig. 12

White and Scalapino